Energy Advances

ROYAL SOCIETY OF CHEMISTRY

PAPER

View Article Online
View Journal | View Issue

Cite this: *Energy Adv.*, 2024, 3, 2245

Comparative evaluation of the power-to-methanol process configurations and assessment of process flexibility†

Siphesihle Mbatha,*[ac] Xiaoti Cui,[e] Payam G. Panah,[e] Sébastien Thomas,[b] Ksenia Parkhomenko,[b] Anne-Cécile Roger,[b] Benoit Louis,[b] Ray Everson,[c] Paulo Debiagi,[f] Nicholas Musyoka[f] and Henrietta Langmi[d]

Received 30th June 2024,
Accepted 13th July 2024

DOI: 10.1039/d4ya00433g

rsc.li/energy-advances

This paper compares different power-to-methanol process configurations encompassing the electrolyser, adiabatic reactor(s) and methanol purification configurations. Twelve different power-to-methanol configurations based on direct CO_2 hydrogenation with H_2 derived from H_2O-electrolysis were modelled, compared, and analysed. A high temperature solid oxide electrolyser is used for hydrogen production. A fixed bed reactor is used for methanol synthesis. The aim of the paper is to give detailed comparison of the process layouts under similar conditions and select the best performing process configuration considering the overall methanol production, carbon conversion, flexibility, and energy efficiency. ASPEN PLUS® V11 is used for flowsheet modelling and the system architectures considered are the open loop systems where methanol is produced at 100 kton per annum and sold to commercial wholesale market as the final purified commodity. Further optimization requirements are established as targets for future work. Three options of power-to-methanol configuration with methanol synthesis from CO_2 hydrogenation are proposed and further evaluated considering process flexibility. From the evaluation, the series–series based configuration with three adiabatic reactors in series performed better in most parameters including the flexible load dependent energy efficiency.

1. Introduction

Investment in renewable energy has been resilient to the Covid-19 pandemic.[1] With the ongoing transition to renewable energy sources particularly variable solar and wind, and the need for cleaner fuel derivatives, chemical energy storage stands central as the best potential solution to meet these sustainability goals. Methanol is a versatile chemical intermediate and due to its ease in handling, it is a robust renewable hydrogen carrier.[2–6] A recent study by Hank *et al.* investigated the potential to transport renewable hydrogen using methanol, ammonia, liquid organic hydrogen carriers and methane.[3] The study reiterated the significant potential of methanol to transport a large amount of green hydrogen over long distances.[3] The fact that various value-added downstream chemicals can be produced from methanol (*i.e.*, the power-to-fuels), its ease in handling and the fact that it can be used directly in the fuel cells to produce electricity (*i.e.* the power-to-power architecture) make it attractive.

Considering plant-to-planet analysis of green methanol *via* using the planetary boundaries tool, González-Garay *et al.* discovered that the potential damage that green methanol can cause to the freshwater use and nitrogen and phosphorus flow is negligible when compared to the positive effects it will have on energy imbalances, CO_2 emission reduction and ocean acidification.[7,8] According to Moioli *et al.* the hydrogen stored in methanol and methane processes is 85.3% and 78.2%, respectively, thus indicating the good storage potential of methanol.[4] However, the methanol economy requires

[a] *HySA Infrastructure Centre of Competence, Centre for Nanostructures and Advanced Materials (CeNAM), Chemicals Cluster, Council for Scientific and Industrial Research (CSIR), Pretoria 0001, South Africa. E-mail: siphe.mbatha94@gmail.com*
[b] *Institute of Chemistry and Processes for Energy, Environment and Health (ICPEES), UMR 7515 CNRS-University of Strasbourg, 25 rue Becquerel, Strasbourg 67087 Cedex 02, France*
[c] *Centre of Excellence in Carbon Based Fuels, School of Chemical and Minerals Engineering, Faculty of Engineering, North-West University, Private Bag X6001, Potchefstroom, 2531, South Africa*
[d] *Department of Chemistry, University of Pretoria, Private Bag X20, Hatfield, 0028, South Africa*
[e] *Department of Energy, Aalborg University, Pontoppidanstr. 111, 9220 Aalborg, Denmark*
[f] *Nottingham Ningbo China Beacons of Excellence Research and Innovation Institute, University of Nottingham Ningbo China, Ningbo 315100, P. R. China*

† Electronic supplementary information (ESI) available. See DOI: https://doi.org/10.1039/d4ya00433g

favourable policy directions.[4–6] In this front, the majority of countries in the European Union (EU) as well as China have already announced ambitious plans to develop commercial scale renewable methanol plants by 2030.[5] Renewable Energy Directive II (RED II) of the EU requires that 14% of renewable energy derived fuels, including green methanol, be part of the transport sector by 2030.[9]

1.1. Recent progress in the PtMeOH system level evaluation

Growing efforts are devoted to the so-called PtMeOH chain as a candidate process for sustainable methanol production *via* CO_2 valorisation and with hydrogen produced from renewable energy resources, *e.g.*, wind and solar, *via* the electrolysis route.[10–16] Electrolysis technologies encompass alkaline water-based electrolysers (AWE), polymer exchange membranes (PEM) and solid oxide electrolysers (SOEC). Numerous studies have evaluated the energetic and techno-economic feasibility of PtMeOH.[2,3,17–24] Rivera-Tinoco *et al.* deduced that SOEC-based PtMeOH has a higher energy efficiency ($\sim$54.8%) than PEM-based PtMeOH.[21] Hank *et al.* evaluated the transport potential, techno-economics, and energy efficiency of PEM-based PtMeOH and deduced that the process has an energy efficiency in the range of 40–44% comparable to the power-to-methane process.[3] Zhang *et al.* evaluated the techno-economics of the SOEC-based biomass-to-methanol process and deduced that an energy efficiency of 66% can be achieved from this process and highlighted a trade-off between the system efficiency and its production cost.[22] However, biomass-based processes are limited by biomass feedstock availability.[20] Zhang *et al.* investigated the techno-economic optimization of the SOEC-based PtMeOH process and similarly observed that there is a trade-off between the energy efficiency and the production costs.[22] Bos *et al.* investigated the techno-economics of a 100 MW wind-based PtMeOH plant with hydrogen produced from AWE and concluded that the process has an energy efficiency of 50%.[17] Al-Kalbani *et al.* compared the environmental performance of fossil fuel-based and renewable energy-based PtMeOH, and their findings depicted that renewable energy-based PtMeOH is attractive from an environmental perspective.[18] The main conclusion from these studies points to high energy demands and high hydrogen production and electrolyser capital costs as the major techno-economic feasibility barriers.[3] The availability of power determines the quantity of hydrogen that can be produced and therefore the optimal capacity and system configuration.[7,17] It also emanates from these studies that the SOEC is an attractive technology from the perspective of energy efficiency and for coupling with exothermic processes such as the methanol production process, although further improvements in the SOEC technology (*e.g.* flexibility) are still required to make its application in renewable PtMeOH more competitive.

On the other hand, these studies highlighted the required improvements in carbon capture technologies, particularly from the confines of energy penalty and cost reduction.[7,17] According to Bos *et al.*, the methanol synthesis loop is dominated by feed compression and the key to optimizing the costs and productivity is to find the favourable ratio between the reactor size(s) and compression requirements such that the reactor operation pressure and cost of compressors remain optimized.[9,17] The latter approach is limited by the trade-offs between pressure (*i.e.* feed compression duties) and conversion due to equilibrium.[7] An alternative is to reduce the recycle compression by increasing the single pass conversion, but according to González-Garay *et al.* and Alsuhaibani *et al.* this strategy has limited impact on profitability relative to decreasing the overall reactor pressure.[7,23] Thus efforts in finding cheap and easy to scale catalysts that operate efficiently at lower pressures ($<$50 bar) shall not cease and their effects will become more dominant ($\sim$24.4% share of the total costs) when power-to-methanol is already economically feasible.[7] Furthermore, a combination of economically effective yield and pressure needs to be identified.[7]

It is also evident from the highlighted studies that, recently, the system level optimization has emerged as a new paradigm shift needed to improve the economics of the process.[24–29] To accelerate technology readiness and techno-economic improvement of PtMeOH, several demonstration projects have been implemented and some are being planned.[26] Nonetheless, availability of data from demonstrated systems remains scarce and difficult to access. On the other hand, modelling efforts in this direction have thus far been directed to a single objective or only two objectives, *i.e.* energy efficiency and production costs. Thus, optimized process flowsheets that enhance the CO_2 and H_2 conversions, energy efficiency, economics of the process (lowering production costs and/or capital), and flexibility and reduce CO_2 emissions and system complexity are required.[3] Due to low conversion of the direct CO_2 hydrogenation over Cu/ZnO/Al_2O_3, GhasemiKafrudi *et al.* optimised the process recycle flow to improve the performance.[24] They considered different process parameters, including temperature, pressure, and GHSV, to reduce the recycle, energy consumption and greenhouse gas emissions of the CO_2 hydrogenation process. Furthermore, GhasemiKafrudi *et al.* investigated the effect of changes in the hydrogen injection as make-up gas, the use of two reactors, inert gases, moisture in the feed, the use of dry hydrogen and the recycle stream on methanol yield.[24] Their results showed that having two reactors with intermediate dehumidification in series and adding hydrogen as make-up gas at the inlet of the second reactor increases the methanol yield by a factor of 1.8.[27] However, the authors also deduced that if one reactor with recycle is used, the resultant methanol yield is almost double when compared to the case of one reactor with no recycle.[24] Finally, GhasemiKafrudi *et al.* concluded that by just modifying the catalyst type and total amount (slightly decreasing it, in their case, to a total amount = 865 kg) and increasing the inlet temperature (*e.g.* in their case to 209 °C), the recycle flow reduces by almost 38%.[24] Moioli *et al.* and Lee *et al.* have already established that for CO_2 hydrogenation on a Cu/ZnO/Al_2O_3 based catalyst, and for both small scale and commercial scale ($\sim$100 kton per annum), three cascade fixed-bed reactors are optimal.[4,14] Lee *et al.* deduced that a configuration with three reactors in series,

having intermediate cooling and separation of methanol/H_2O between the reactors, is optimal in terms of profit (from a deficit of \$4.3 to \$2.5 profit per ton) and CO_2 conversion ($\sim$52%).[14] However, Lee *et al.* using process superstructure and techno-economic optimization methods investigated the best configuration that optimizes the profit for the two step CO_2 hydrogenation process in which both CO_2 and CO participate as carbon sources in hydrogenation reactions to methanol and focused only on the synthesis and purification step instead of the direct CO_2 hydrogenation process as will be considered in this study.[14] Furthermore, the superstructure optimisation approach tends to discard the suboptimal flowsheets following set objectives and constraints without giving further details as to why the suboptimal process underperforms and the possibility of improving it further.[27]

More recently, Chiou *et al.* investigated six different configurations for the PtMeOH focusing on single stage and multi-stage series reactor(s) connections with adiabatic and non-adiabatic (with co-current cooling) reactor type.[28] Their study focused on design, optimisation, control, techno-economics, and environmental aspects of the process considering a small scale (20 kton per year) plant capacity. They reached the conclusion that two reactors with first stage non-adiabatic (with co-current cooling) and second stage adiabatic reactor type in series with inter-stage cooling and separation of methanol and water was more economically attractive (with a minimum selling price of methanol of 998 US\$ per ton and carbon tax of 283 US\$ per ton) and showed better performance. From this, they devised a control strategy aimed at handling the throughput and compositional disturbances for their proposed configuration. The rejection of two kinds of compositional disturbances, *i.e.* (i) 5% N_2 and (ii) H_2 impurity, was investigated. Their control strategy allowed the rejection of both compositional disturbances within 5 h. It was noted that an increase in N_2 impurity composition deteriorates the reaction kinetics and increases the purge rate which reduces methanol production rate with higher loss of CO_2 and H_2. Thus, to maintain the single pass conversion, the H/C ratio will have to be increased. The authors however did not investigate any full integrated process with the electrolyser, parallel–series configuration, and the three-stage reactors with intercooling, nor the detailed load change flexibility of their system.

1.2. Recent progress in PtMeOH process flexibility

Production processes are prone to stochastic variation, for example, in system input parameters, internal process parameters and environmental factors.[30] A degree of process flexibility helps to deal with these challenges. The level of process flexibility affects the economic gain of the process and the selection of the right conditions (*i.e.* parameters, location, capacity, *etc.*) in which the process operates economically.[30–33] In this paper, flexibility refers to the ability to handle the changes in the feedstock composition/flow or adjustments to other changing boundary conditions in order to adapt the plant operation to the changes in the energy or material supply.[34] It is well known that the electrolyser, in particular the PEM type which is suitable for rapid start-up, can provide good flexibility.[32,35,36] Lange *et al.* recently gave a good technical review of the state-of-the-art of the electrolyser technology's flexibility including the SOEC technology which will be considered in this study due to its high efficiency.[36] Lange *et al.* deduced that the SOEC can provide a broad range of load flexibility (−100% to 100%), but this is countered by its long cold-startup time ($\sim$60 min).[36] However, efforts are being made on the front of improving the performance of the materials for the SOEC cells/stack to allow more flexibility and shorten the start-up time without incurring severe cell damage.[36,37] The recent results such as in the work of Li *et al.* showed great potential of the future of the SOEC in handling flexibly the intermittent renewable energy supply with reduced start-up time.[37]

In a coupled electrolysis-methanol synthesis system, intermediate gas (hydrogen and CO_2) storage under intermittent conditions may be needed unless the reactor operates flexibly. If the reactor has a wide tolerance to variations in the operational parameters, it is referred to as the load flexible reactor. The load range of the catalytic reactor is a function of chemical reactions, transport rate, catalysts, and reactor design.[32] The attainable load flexibility of the methanol reactor section has not been investigated, at least intensively.[31–33] At present, to the author's knowledge, only INERATEC Gmbh has expressed interest to investigate and scale-up the flexible modular micro-structured reactors. Considering the case of variable renewable energy-based processes, flexibility is typically achieved by over-sizing the main process equipment to account for variability in the load. The size of the equipment directly influences the propagation of disturbances within the unit, and the bigger the size, the smaller the influence of disturbances on process variables. However, the load range of the reactor is also limited by operational issues such as maximum temperature rise and ability to achieve autothermic control, in which the reactor outlet is used to heat the feed (*via* the feed-effluent heat exchanger concept).[31] The heat of reaction is, with careful heat management, generally enough to heat the feed to the methanol synthesis reactor(s) and/or distillation column, thus allowing the system to operate autothermally, *i.e.* achieving energy self-sufficiency without external heating/cooling. In cases where the reactor feed stream is not sufficiently heated, the reaction rate will decrease and thus leads to low outlet temperature, which in effect results in lower inlet temperature and consequently the reaction halts completely. According to the study on fixed bed reactors performed by Zimmermann *et al.*, with methane as an example, the step responses typically implemented by switching from one steady state to another were found to be the worst-case load change policy due to the existence of unfavourable behaviour such as temperature overshoot and conversion drops.[38] Appropriate design of the network structure can help achieve necessary flexibility without additional oversizing of the equipment.[39] According to Grossmann and Morari, flexibility cannot be simply achieved by *ad hoc* addition of equipment or oversizing but by systematic design techniques.[40]

Rinaldi and Visconti assessed the steady state and transient performances of a multi-tubular fixed bed reactor for methanol production from biogas.[41] Their modelled system had a methanol synthesis reactor and a flash unit, and accounted for the unconverted gas recycle. The novelty of their conceptual work was to assess the possibility to run a multi-tubular methanol synthesis reactor flexibly, *i.e.*, using carbon dioxide from biogas and renewable H_2 in order to increase methanol productivity when the process is economically feasible. In their work, the investigation of the methanol synthesis multi-tubular reactor is conducted considering the impacts, on methanol productivity, temperature profile and transient behavior, of the two operating conditions, *i.e.* (i) when the cost of green hydrogen is high, the excess of CO_2 in the biogas is vented and the reactor is fed with CO_2–lean syngas only; (ii) conversely, when affordable renewable H_2 is available, CO_2 is co-fed into the reactor along with this affordable green H_2.[41] These authors compared 1D and 2D models in terms of their ability to better predict the temperature and production profile.[41] They deduced that the concerned reactor manages well both operating conditions with steady state reached within a few hours when switching from one condition to another and that 2D models are better suited to predict the temperature and methanol production profile. Moreover, they also highlighted that reducing the number of tubes (equivalent to reducing the catalyst amount and measured using GHSV) instead of the reactor length is preferred especially for small scale processes. Reducing the length of the reactor can lead to unacceptable hot-spots from the resultant worsening of the convective heat transfer and reduced selectivity to methanol. When the length of the reactor is shortened, the thermal peak is achieved at higher temperatures, and the gaseous stream remains mostly in the kinetic regime near the end of the reactor.[41] This was prevalent when syngas was fed with and without co-feeding CO_2 and H_2, and when the length of the reactor was decreased below half (up to $\frac{1}{4}$) of the original length.[41]

Furthermore, Svitnič and Sundmacher investigated the effect of flexibility of the methanol synthesis process on the levelized cost of methanol (LCOM).[42] In their finding, the flexibility gains are most prominent for the designs with a single source of renewable energy (either solar or wind) leading to reduction of costs of more than 10%. This gain is significantly reduced for the design with combined solar and wind resources, as the complementary availability of renewable resources allows better sustaining stable operation of the chemical processes, reducing the influence of flexibility to 5.1%. Moreover, the authors deduced that the flexible operation of the methanol synthesis has a stronger effect on the reduction of LCOM, where for the design with a single renewable resource it delivers a roughly 4-times larger reduction of LCOM.

More recently, Qi *et al.* investigated different strategies for flexible operation of the power-to-X processes coupled with renewables using PtMeOH as a reference.[33] The strategies they compared involved the use of the energy buffers, *i.e.* the hydrogen intermediate storage, liquid CO_2 energy storage as a Carnot battery, and Li-ion battery storage. In considering these strategies, they generated nine process configurations with islanded, grid-assisted only, and grid-assisted bidirectional connections for allocation of energy. Qi *et al.* considered a combination of solar and wind energy as well as grid electricity purchase.[33] The configurations with grid-assisted bidirectional connections resulted in the most cost-effective way for flexible operation of the power-to-X and the lowest levelized cost ($\sim$479.4 US$ per ton) was achieved when the Carnot battery was used. However, this is still more expensive than methanol production from autothermal reforming of natural gas which can reach a cost of 285.6 US$ per ton, thus indicating that further research and development is needed to make renewable methanol production cost-competitive with other methods. In addition, some trade-offs were observed amongst the performance indexes which indicate that there is no single best solution but rather more case dependent solutions. Moreover, studies are required that incorporate the dynamic modelling of the energy buffer and the electrolyser to account for the factors such as the time varying energy efficiency and the limitations on power ramp-up.[33] Process operation can influence the design of the process and hence the flowsheet. Compared to investigations focusing on methanol synthesis catalyst improvements, studies focusing on PtMeOH reactor design, process configurations and process flexibility are very few. The objective of this paper is to model and compare different PtMeOH process layouts under steady state and dynamic conditions with the consideration of their process flexibility.

1.3. Statement of originality

The originality of the work in this paper lies in the comparative flexibility analysis of different integrated methanol synthesis system configurations comprising parallel–series and series–series connections. Twelve integrated flowsheets (including co-electrolysis and the electrified reverse water gas shift (e-RWGS) system) based on SOEC, methanol synthesis and purification steps are contrasted to assess their performance in terms of energy efficiency, production rate, and material conversion. In addition, the better performing CO_2 hydrogenation-based flowsheets are assessed under dynamic mode for their flexibility and to answer the following questions:

(1) What is the feasible (with minimum sophisticated equipment) load-change flexibility window?

(2) What is the effect of the load change in the parallel–series and series–series-based configurations?

(3) How do the energy efficiency and conversion in the mentioned flowsheet design change with the change in the load?

Candidate PtMeOH configuration(s) with methanol synthesis from CO_2 hydrogenation is proposed. Furthermore, optimization requirements are established as targets for future work. The paper is structured as follows: Section 2 gives the base content and approach to modelling, Section 3 gives the detailed results and discussion, Section 4 concludes the work and Section 5 gives recommendations for future work.

2. Process synthesis and modelling

Twelve different flowsheets are synthesized and simulated (see Table 6 and Section A2 in the ESI† for more details) under steady state conditions in Aspen Plus® V11, and out of the twelve, three are selected for flexibility assessment under the Aspen Dynamics V11 platform. Table 1 shows the assumptions pertaining to feed conditions. The system's capacity is designed to store about 162 MW of renewable electricity from either wind or Solar PV farm. This is of the scale of a commercial size plant.[43–45] For all flowsheets, the SOEC configuration was left unchanged; however the methanol synthesis section configuration was modified to generate twelve different process configurations. Following the findings of Samimi *et al.* on the possibility to enhance the production rate of methanol with the exclusion of inert gases in the feed, inert gases are neglected in this study.[46]

The exclusion of inert gases allows setting the lowest possible purge as detected by the system control parameters.[9,47] The recycle ratio is an effective control parameter of the process (particularly the reactor) productivity and temperature.[46] It is also critical to highlight that the dynamic modelling of the SOEC to ascertain its capability is beyond the scope of this work. Rather the focus on dynamic modelling is placed on the downstream reactor configurations to establish their flexibility.

2.1. SOEC modelling

The electrochemical model to simulate the SOEC was implemented in ASPEN PLUS® V11 in the FORTRAN routine with the use of design specifications and calculator functions. Water, sweep gas (oxygen) and electricity are the primary feeds to the SOEC unit. The thermodynamic model used in modelling the electrolysis is the Redlich–Kwong–Soave equation of state (EOS) with modified Huron–Vidal mixing rules (RKSMHV2).[48–50] The main electrochemical model is a function of product species, which are electrochemically active, *i.e.* i = H_2. The net voltage is expressed by eqn (1):

$$E_i = E_{nerst,i} + E^{her}_{act,i} + E^{oer}_{act,i} + E_{ohm,i} + E_{mic,i} \quad (1)$$

Table 1 Feed conditions

Raw materials	Temperature (°C)	Pressre (bar)	Flowrate (kmol h^{-1})	Composition (mol%)
CO_2	25	1.0	401	100
H_2O	25	1.0	1232	100
Sweep gas (oxygen)	25	1.0	31	100
Steam electrolysis product H_2 feed stream to MEOH unit				
H_2	35	5.0	1212.5	98.8
H_2O	35	5.0	14.3	1.2
Co-electrolysis product syngas feed stream to MeOH unit				
H_2	35	5.0	1212.5	74.3
CO_2	35	5.0	105	6.4
CO	35	5.0	296	18.1
H_2O	35	5.0	19.3	1.2

where $E_{nerst,i}$ is the Nernst potential, $E_{act,i}$ refers to the over-potential due to activation of electrochemical reactions, $E_{ohm,i}$ refers to the ohmic over-potential and $E_{mic,i}$ is the interconnect voltage loss. The system is assumed to operate at thermoneutral stack voltage and under steady state, and thus eqn (2) is used as the main equation to calculate the thermoneutral energy.

$$E_{tn} = \frac{\Delta H_r}{I_{tot}} = E_i \quad (2)$$

where ΔH_r is the heat of reaction and I_{tot} refers to the total current (A). According to Giannoulidis *et al.*, it is advantageous from the perspective of the SOEC energy efficiency to operate the unit at low pressure (<10 bar).[2] For the selected operating conditions, thermoneutral operation is achievable.[45,51] Generally, the planar O-SOEC is operated in the temperature range of 150–950 °C and pressure range of 1–8 bar.[2,52,53] The SOEC operating under co-electrolysis conditions can already produce syngas at a ratio of 1.5 to 3.5.[53] The SOEC unit capacity is designed for 109 MW considering the SOEC operating under steam electrolysis only. However, for the co-electrolysis based SOEC unit capacity, only 134 MW is required to produce the syngas given in Table 2. Table 2 shows the input parameters used in the modelling of the SOEC unit. Generally operating the SOEC at higher temperature lowers the electricity requirements and hence increases the energy efficiency. The choice of temperature is a reasonable compromise between allowable concentration over-potential, ohmic over-potential and possibility of achieving thermo-neutral point operation.

Typically, near or at the thermoneutral point, high electrolysis efficiency and minimum sweep gas flowrate are achievable.[2] This makes operating the electrolyser at the thermoneutral point attractive.[2,54,55] Fig. 1 illustrates the SOEC model flowsheet for steam electrolysis implemented in ASPEN PLUS.

Fig. 2 illustrates the SOEC model flowsheet for co-electrolysis implemented in ASPEN PLUS. For steam electrolysis (see Fig. 1), demineralized water (stream Fresh Water feed) is first pumped to increase its pressure to SOEC operating pressure, then vaporised and superheated in a cascade of heat exchangers, and mixed (*via* CATHOD-M) with cathode feed recirculation (*i.e.* stream H_2-Recycle stream) which contains

Table 2 SOEC operating conditions and parameters for steam and co-electrolysis

Parameter	Value	Unit
Steam inlet temperature of SOEC	850	°C
Air inlet temperature of the SOEC reactor	850	°C
SOEC stack temperature	850	°C
Reactant utilization	70	%
H_2 cathode inlet recycle	10	%
Operation pressure	5.0	Bar
Stack consumption	29.7	kW h kg H_2^{-1}
Hydrogen production	2827	kg h^{-1}
Syngas production	15 360	kg h^{-1}
Syngas ratio (methanol feed)	2.2	—
LHV of syngas	25	MJ kg^{-1}

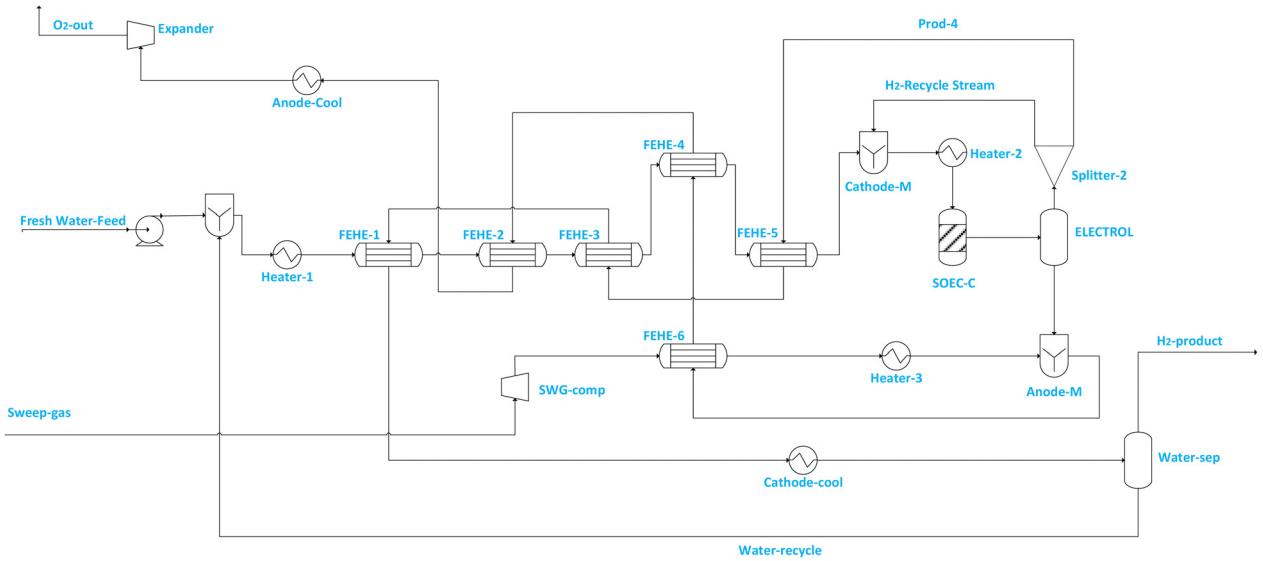

Fig. 1 Illustration of the SOEC unit used for steam electrolysis in ASPEN PLUS®.

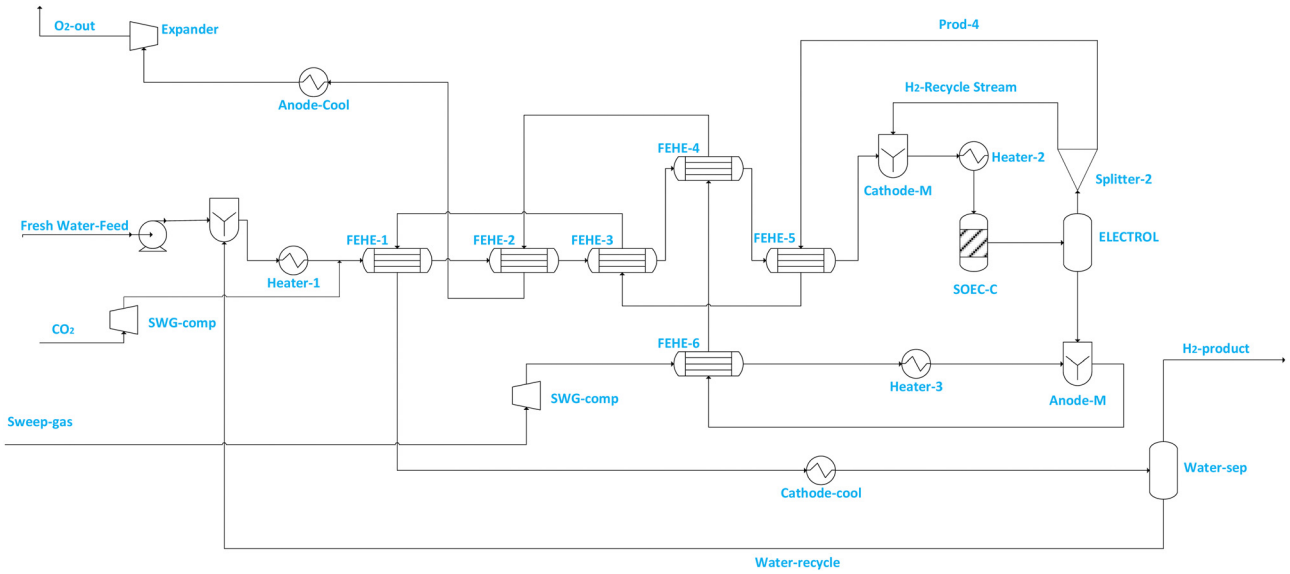

Fig. 2 Illustration of the SOEC unit used for co-electrolysis in ASPEN PLUS®.

10 mol% of hydrogen.[56–60] The hydrogen fraction is recycled to prevent electrode (*i.e.* Ni-YSZ) re-oxidation.[56] The composition of steam in the SOEC feed (*i.e.* stream SOEC-FEE) is maintained above 90% to prevent starvation at the electrode, which may cause cell damage. The SOEC cathode is modelled using RSTOIC, using the conditions in Table 2 and the feed steam utilization factor (*i.e.* in the SOEC-C unit) is assumed to be 70%. The product stream from the SOEC-C containing oxygen, hydrogen and unconverted water of the SOEC cathode (SOEC-C) is separated in the electrolyte (*i.e.* represented by ELECTROL) into two product streams. The overhead product stream from the ELECTROL contains only water and hydrogen, and it is split (*via* Splitter 2) into product stream containing wet hydrogen (*i.e.* stream PROD-4) and recycle stream (*i.e.* H2-Recycle stream). Stream PROD-4 is used to pre-heat the feed stream, and it is ultimately cooled and fed to the separator block (*i.e.* WATER-SEP) in which a significant quantity of water (*i.e.* stream Water-recycle) is removed (discharged or recycled) and wet hydrogen at 98.8 mol% is fed to the methanol synthesis section. The bottom product stream from ELECTROL contains only oxygen. The cascade heat exchanger network is used to recuperate the heat from the effluent streams for the purpose of generating superheated steam at cheaper cost. Sweep gas (*i.e.* stream Sweep-gas) is assumed to contain only oxygen and is first compressed (*via* SWG-comp) to SOEC pressure, heated (*via* FEHE 2, HEATER 2) to SOEC temperature and fed to the

anode side (*i.e.* modelled as ANODE-M) of the SOEC unit to remove the oxygen produced during electrolysis. The removed oxygen is then used in the cascade heat exchanger to preheat steam, after which it is cooled and expanded to atmospheric conditions before being discharged or alternatively sold or sent to another process (*i.e.* stream O2-out).

The use of oxygen (recirculated) as a sweep gas manages possible overshoot in the over-potential and therefore allows for higher energy efficiency operation of the electrolyser. During the start of the process, oxygen is assumed to come from its storage tank, while during operation it can be recirculated from the anode with some stored or sold to end users. It is noted beforehand that the use of oxygen may increase the exergy destruction, but the difference between the exergy efficiency when steam or air is used as sweep gas is expected to be marginal, with steam as sweep gas having the exergy efficiency which is ~1% more than that of oxygen.[47,57] In addition, using oxygen as a sweep gas allows the production of pure oxygen which can be sold to the market.[47,57]

2.2. Steady state: reactors and separation modelling

Both CO_2 and H_2 feed streams are compressed to 78 bar using multiple compressors each with an isentropic efficiency of 75% for the steam electrolysis-based PtMeOH. For the co-electrolysis-based system, the syngas feed is compressed in a two-stage compression system to 78 bar with the same isentropic efficiency. Considering safety aspects as it would be necessary in real plants, the compression ratio is kept at 3 and inter-stage cooling is included. The temperature of the feed stream to reactor(s) was set to 210 °C.[61] The inlet temperature is in a typical range of an optimised industrial methanol reactor;[61] a higher inlet temperature can result in a higher outlet temperature and a lower methanol yield, particularly for the adiabatic reactor(s). In addition, the lower limit for allowable inlet temperature is defined by the catalyst, and for the commercial copper-based catalyst it is around 190 °C.[62] A commercial $Cu/ZnO/Al_2O_3$ catalyst is used in this study. The reactor(s) is modelled as an adiabatic reactor(s). Table 3 gives the properties of the adiabatic reactor(s) modelled as a plug-flow (RPLUG) and those related to the catalyst. Adiabatic reactors have lower cost relative to the water-cooled and gas-cooled reactors due to their simple structural designs.[62] The advantage of adiabatic reactors is that under nominal steady state conditions their size is very small, and thus their over-sizing slightly affects the capital cost.[63–65] This indicates their potential in small scale PtMeOH processes as well.[62] The reactor size was selected to be large enough such that the effluent from the reactor is near equilibrium.[47] The Redlich–Kwong–Soave equation of state with modified Huron–Vidal mixing rules (RKSMHV2) was used to model the reactor(s) and auxiliaries and to calculate the thermodynamic properties of the streams (refer to Section A1 of the ESI†). After separation of methanol and water using a flash drum, a recycle stream was purged up to 0.1% for all flowsheets (see Section A4.2 of the ESI† for the sensitivity on recycle fraction). In line with the work of Cui *et al.*, the small purge of 0.1% was set, which aims to minimize the CO_2 emission for green methanol production.[66] As observed by Cui *et al.*, using a larger purge ratio can result in lower flow rate of the recycle stream as well as a smaller reactor size but a higher CO_2 loss. It was also observed by Cui *et al.* that a value lower than 0.1% may cause convergence problem.[66] For the syngas (co-electrolysis-based system), the purge stream after methanol separation and recycle was set to 1.3%.

Table 3 Adiabatic plug-flow reactor(s) operating conditions

Parameter	Value	Unit
Tube diameter	3–5	m
Tube length	3–12	m
Reactor inlet pressure	74–75.7	bar
Catalyst particle density	1775	kg m^{-3}
Bed porosity	0.5	—
GHSV	4000–7300	h^{-1}

2.2.1. Reaction kinetics. Industrially, methanol is synthesized from syngas following the three main equilibrium reactions as expressed by eqn (3)–(5) over an industrial $Cu/ZnO/Al_2O_3$ catalyst. However, it has been recently agreed and demonstrated that methanol can also be produced from a feed with pure CO_2/H_2, *i.e.*, *via* eqn (3) only even though the actual reaction mechanism and carbon source for methanol remain an active subject of debate.[10–13]

$$CO_2 + 3H_2 \leftrightarrow CH_3OH + H_2O \quad \Delta H_{298K} = -49.43 \text{ kJ mol}^{-1} \tag{3}$$

$$CO_2 + H_2 \leftrightarrow CO + H_2O \quad \Delta H_{298K} = +41.12 \text{ kJ mol}^{-1} \tag{4}$$

$$CO + 2H_2 \leftrightarrow CH_3OH \quad \Delta H_{298K} = -90.55 \text{ kJ mol}^{-1} \tag{5}$$

Following the Le Chatelier's principle, higher methanol yields are favoured at lower temperatures and higher pressures. However, for the reason of enhancing kinetics, temperatures in the range of 200–300 °C are used as well as high pressure ranges of 50–100 bar over the commercial $Cu/ZnO/Al_2O_3$ catalyst. The reverse water gas shift reaction (eqn (4)) is the only endothermic reaction among the three main reactions and therefore gets promoted as temperature increases. This reaction increases the amount of water generated in the case when pure CO_2/H_2 is the main feed. This lowers the selectivity to methanol and the catalyst activity. As a result, significant research efforts are devoted to the CO_2 hydrogenation to methanol process, mostly to improve the catalyst conversion and selectivity.[14,15] However, the commercial $Cu/ZnO/Al_2O_3$-based catalyst is likely to remain the best possible for some time due to its ability to achieve the highest yield, its low costs, and high stability.[16] Ruland *et al.* established, through dynamic experimental conditions relevant to power-to-methanol (PtMeOH), that the industrial $Cu/ZnO/Al_2O_3$ is highly stable for conditions of chemical energy storage with hydrogen produced from fluctuating renewable energy sources, indicating its relevance for application in PtMeOH.[16] Besides the challenges of optimizing the catalyst beyond what the commercially available catalyst can achieve to promote CO_2/H_2 to methanol, this

reaction is attractive from an environmental perspective in that a significant quantity of CO_2 can be recycled, and in addition it is less exothermic, thus rendering ease of heat management in the reactor, and involves fewer by-products' formation. For these reasons and following the most recent kinetic analysis such as in the work of Nestler *et al.*, Slotboom *et al.*, and de Oliveira Campos *et al.*, who deduced that the contribution of the CO hydrogenation to the overall methanol production is negligible at a high CO_2/CO feed ratio, in this work only reactions (3) and (4) are considered in the modelling of the methanol synthesis.[67–69]

The kinetic model used in this study was presented in the work of Van-Dal and Bouallou,[64] which originated initially from the model of Bussche and Froment.[63,65] The model assumes methanol production from CO_2 hydrogenation (*i.e.*, eqn (2)) in the presence of RWGS as a competing reaction (eqn (4)) and in the absence of diffusional limitations. Thus, the effectiveness factor equals 1. The kinetic model is based on the Langmuir Hinshelwood Hougen–Watson (LHHW) kinetic model formulation and is expressed by eqn (6) and (7):

$$r_{CH_3OH} = \frac{k_1 P_{CO_2} P_{H_2} - k_6 P_{H_2O} P_{CH_3OH} {P_{H_2}}^{-2}}{\left(1 + k_2 P_{H_2O} {P_{H_2}}^{-1} + k_3 {P_{H_2}}^{0.5} + k_4 P_{H_2O}\right)^3} \mathrm{kmol\,kg_{cat}^{-1}\,s^{-1}} \quad (6)$$

$$r_{RWGS} = \frac{k_5 P_{CO_2} - k_7 P_{H_2O} P_{CO} {P_{H_2}}^{-1}}{1 + k_2 P_{H_2O} {P_{H_2}}^{-1} + k_3 {P_{H_2}}^{0.5} + k_4 P_{H_2O}} \mathrm{kmol\,kg_{cat}^{-1}\,s^{-1}} \quad (7)$$

where k_i were calculated for implementation in ASPEN PLUS V11® using eqn (8) and these are tabulated in Table 4.

$$\ln k_i = A_i + \frac{B_i}{T} \quad (8)$$

Table 5 presents the main parameters of the distillation column which was modelled as RadFrac in ASPEN PLUS V11®.

All flowsheets used the same conditions, except the distillation column (DC) in flowsheet 2 in which the boilup ratio was set to 0.9 (lower) to ensure that the methanol purity remains above 99 wt%. NRTL-RK was selected as a property method to model the distillation column and its feed (with pressure $\leq$1.1 bar).

Validation of the kinetic model is presented in Section A2 of the ESI.† The typical catalyst pellets of 6 mm × 4 mm were packed in the catalyst bed and the Ergun equation was used for pressure drop calculation through the catalyst bed. Following process engineering principles, the reactors were sized at constant total reactor(s) volume. A hold-up time of 5 minutes was used in sizing the separators, and the compressor curves were used to model the compressors. Valves were modelled taking into consideration the typical efficiency relations and pressure drops. Thus, in modelling the different systems, the following assumptions were made:

- An adiabatic fixed-bed tubular reactor has been used to convert CO_2 and H_2 into methanol. The overall CO_2, H_2O or H_2 feed is kept constant as in Table 1.
- The kinetics model and its parameters are kept constant. Where there are multiple reactors, the total reactor volume of all the reactors combined is kept constant similar to base case flowsheet 1 with one reactor as shown in Section A3, Fig. S3 and Section A5, Table S10 (ESI†). This keeps constant the total amount of catalyst used in all flowsheets, which is paramount for cost effective comparison.
- The reactor feed temperature is selected in the optimal temperature range ($210 < T_{in} < 240$) to optimise the temperature profile and conversion in the reactor.[62] Refer to Section A4 (sensitivity-based optimisation) of the ESI.†
- The by-products are negligible, and thus the produced materials in the reactor are methanol, CO, and water.
- Solar PV is used as a source of electricity. In the process, water is used for cooling.
- Catalyst deactivation is negligible.
- The temperature of any flow or equipment is not considered lower than 20 °C, so that there is no need for a refrigerant cycle.
- The operating conditions have been selected with respect to the limitations of the industrial equipment and considering the outcomes of the design sensitivity analysis in Section A4 of the ESI.†
- In the hydrogen stream entering the process, 1.2 mol percent of water is considered.

2.2.2. System configurations. It is important to highlight that all flowsheets comprise a recycle loop, and the SOEC flowsheet was fixed for better comparison. Flowsheets 1 to 6B are shown in Section A3 (ESI†) along with their brief description. To be concise, in this section, only the finally selected flowsheets 7, 7B and 8 are shown as these will be discussed in more detail in the subsequent sections. Table 6 gives the description of the different flowsheets. The selection follows from the comparison with flowsheets 1 to 6B as described in

Table 4 Kinetic parameters rearranged for implementation in ASPEN PLUS V11® as a LHHW model[54,57]

Kinetic parameters	A_i	B_i
k_1	−29.87	4811.2
k_2	8.147	0
k_3	−6.452	2068.4
k_4	−34.95	14 928.9
k_5	4.804	−11 797.5
k_6	17.55	−2249.8
k_7	0.1310	−7023.5

Table 5 Main parameters of the distillation column used for final separation of methanol

Parameter	Value	Unit/basis
Column	RadFrac	—
Number of trays	30	—
Condenser type	Partial-vapor-liquid	—
Reflux ratio	1.5–1.62	mole
Boilup ratio	0.9–1.5	mole
Feeding temperature	80	°C
Operating pressure	1.1	bar

Table 6 Description of different flowsheets, their advantages, and limitations

Process configuration	Description	Advantages	Limitations
Flowsheet 1	This is the base configuration with a single stage adiabatic reactor	• Simple configuration • Less equipment and thus capital investment • Simple start-up process	• Large recycle stream is required for this process • Low single pass conversion • More valuable hydrogen purged
Flowsheet 2	Single stage reactor, with stripper column mounted before the reactor to enhance condensation and separation of methanol from CO_2 and remove water from the wet hydrogen feed	• Help to prevent catalyst deactivation from wet hydrogen • Enhances the separation of dissolved gases from the methanol/water mixture	• Large recycle stream is required for this process • Low single pass conversion • More valuable hydrogen purged
Flowsheet 3	Comprises two adiabatic reactors in series and with intermediate cooling and separation of methanol and water at 45 bar and 35 °C. The other feature of flowsheet 3 is the addition of compressor to the feed of the second reactor to raise the operating pressure of the second reactor to the same pressure as the first reactor in the scheme	• Optimises the pressure to the second reactor and the overall pressure profile to enhance methanol production on the second reactor • Enhances the conversion of the unconverted gases from the first stage • Reduces the recycle stream	• Increased number of equipment means more capital investment • Repeated heating and cooling
Flowsheet 4	It has two reactors in series but with a wash column which uses $C_3H_8O_3$ as a solvent mounted in the position after the reactor followed by separation and two distillation columns in which the first is used for solvent recovery while the second distillation column is used for methanol purification	• This design enhances the driving force of the reaction by eliminating as much as possible water and methanol from the unconverted gases • Enhances the conversion of the unconverted gases from the first stage • Reduces the recycle and compression work	• Increased number of equipment means more capital investment • Increased pressure drop with more reactors, and slightly increased compression • Complexity and additional solvent recovery requirements • Repeated heating and cooling
Flowsheet 5	Closely resembles flowsheet 3 with two reactors in series but with a change in the operation of the intermediate separator which is operated at pressure equal to the reactor pressure to avoid the compression of the feed to the second reactor which comprises unconverted gases and some fraction of methanol	• Reduces compression work and recycle • Enhances the conversion of the unconverted gases from the first stage	• Increased number of equipment means more capital investment • Increased pressure drop with more reactors, and slightly increased compression
Flowsheet 6A	Has two reactors connected in parallel. It also has long recycle to both reactors and therefore a feed (comprising fresh feed and recycle) split at 50% to both reactors	• Increases the residence time in each reactor and thus aims at enhancing the conversion • Reduces the number of intermediate separators • Reduces repeated heating and cooling	• High recycle flowrate • High compression requirements
Flowsheet 6B	Has two reactors connected in parallel. It has a short recycle in which the fresh feed flow is split to 50% and the portion of the fresh feed to the second reactor in flowsheet 6B is mixed with all the recycle of unconverted gases whereas the portion to the first reactor is kept as fresh feed	• Increases the residence time in the first reactor and thus aims at enhancing the conversion • Reduces the number of intermediate separators • Increases the residence time in the first reactor and thus aims at enhancing the conversion	• High recycle flowrate • Relatively poor overall conversion • Removes the recycle as a lever for temperature control in the first reactor especially for part-load operation
Flowsheet 7	Includes two reactors connected in parallel followed by intermediate separation of methanol and series connection with the third reactor and thereafter, recovery of methanol from the recycle using two separators and a further separation of residual gases at low pressure before the distillation column from which the final methanol product flows	• Increased reactant conversion and flexible loading/operation • Reduced compression requirements, and hence potentially improved energy efficiency • Reduced purge stream and hence CO_2 emissions	• Increased number of equipment means more capital investment • Increased pressure drop with more reactors, and slightly increased compression requirement • Complex start-up and shutdown with repeated heating and cooling
Flowsheet 7B	Has almost similar components as flowsheet 7 but the difference is that all reactors are connected in series. The feed to the	• Increased reactant conversion	• Increased number of equipment means more capital investment

Table 6 (*continued*)

Process configuration	Description	Advantages	Limitations
	third reactor is taken from the overall recycle stream and compressed further to boost the pressure	• Reduced compression requirements, and hence potentially improved energy efficiency • Reduced purge stream and hence CO_2 emissions	• Increased pressure drop with more reactors, and slightly increased compression requirement • Complex start-up and shutdown with repeated heating and cooling
Flowsheet 8	Has three reactors connected in series, but the flowsheet is a simplified series connection version of flowsheet 7B. This configuration has no booster compressor for the feed to all downstream reactors except the main recycle compressor feed	• Increased reactant conversion • Reduced compression requirements, and hence potentially improved energy efficiency • Reduced purge stream and hence CO_2 emissions	• Increased number of equipment means more capital investment • Increased pressure drop with more reactors, and slightly increased compression requirement • Complex start-up and shutdown with repeated heating and cooling
Co-electrolysis flowsheet	Has three reactors connected in series, similar to flowsheet 8. The main difference is that the upstream steam-electrolysis step is changed to co-electrolysis mode and thus a fresh feed to the reactor contains syngas with increased CO concentration.	• Existing catalyst optimised for the syngas feed • Co-electrolysis step enhances the energy efficiency of the system • Enhanced conversion with the introduction of CO	• Would practically result in more impurities and difficulties in downstream separation as in the case of the existing industrial syngas systems. • Selectivity to methanol decreases with the increase in the CO/CO_2 ratio
e-RWGS flowsheet	Has three reactors connected in series, similar to flowsheet 8. The main difference is the upstream steam electrolysis step which is coupled e-RWGS and thus leading to fresh feed to the reactor with syngas instead, and increased CO concentration	• Enhanced conversion with the introduction of CO • Existing catalyst optimised for the syngas feed • Higher CO/CO_2 ratio leads to higher methanol production	• Would practically result in more impurities and difficulties in downstream separation as in the case of the existing industrial syngas systems. • Selectivity to methanol decreases with the increase in the CO/CO_2 ratio • Requires separation of water formed from the e-RWGS reactor

the results section (Section 3). Flowsheet 7 illustrated in Fig. 3 includes two reactors connected in parallel followed by intermediate separation of methanol and series connection with the third reactor and thereafter, recovery of methanol from the recycle using two separators and a further separation of residual gases at low pressure before the distillation column from which the final methanol product flows. Flowsheet 7B illustrated in Fig. 4 has almost similar components as flowsheet 7 but the difference is that all reactors are connected in series. Flowsheet 8 illustrated in Fig. 5 has three reactors connected in series, but the flowsheet is a simplified series connection version of flowsheet 7B.

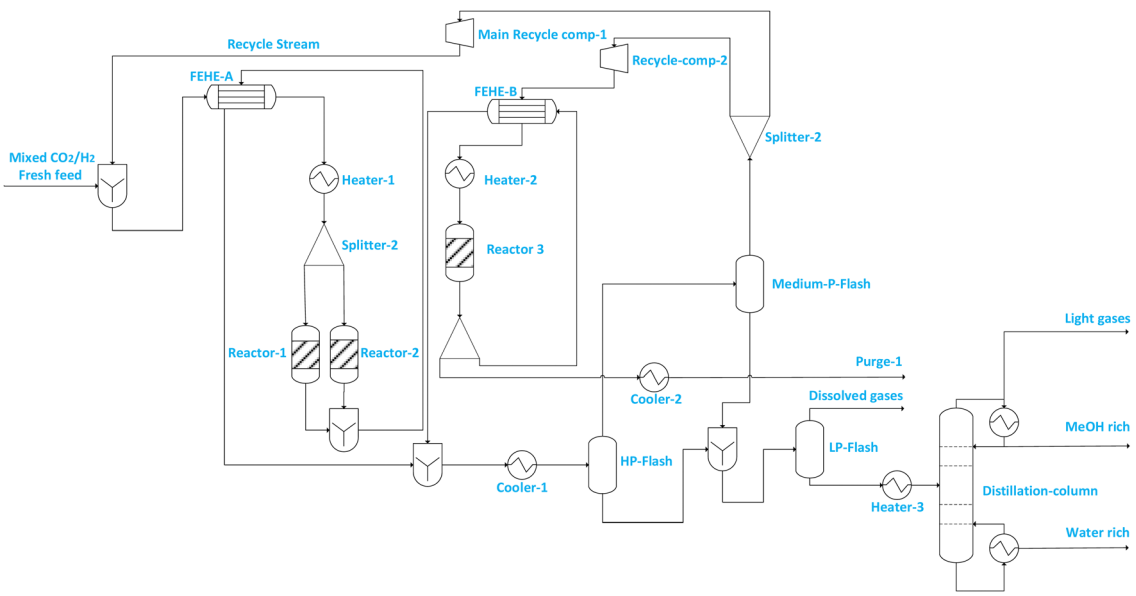

Fig. 3 Illustration of flowsheet 7. This flowsheet features parallel–series configuration of the three adiabatic reactors.

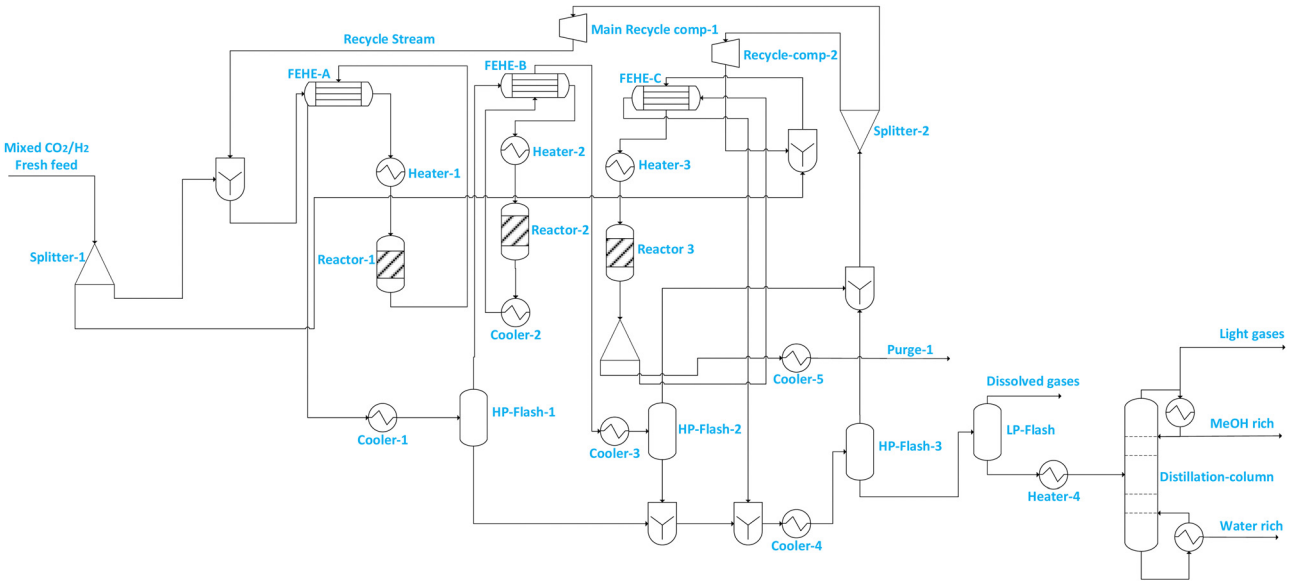

Fig. 4 Illustration of flowsheet 7B. This flowsheet features three reactors in series with intermediate cooling. This features a different feed, product-purge arrangement to the third reactor (reactor 3).

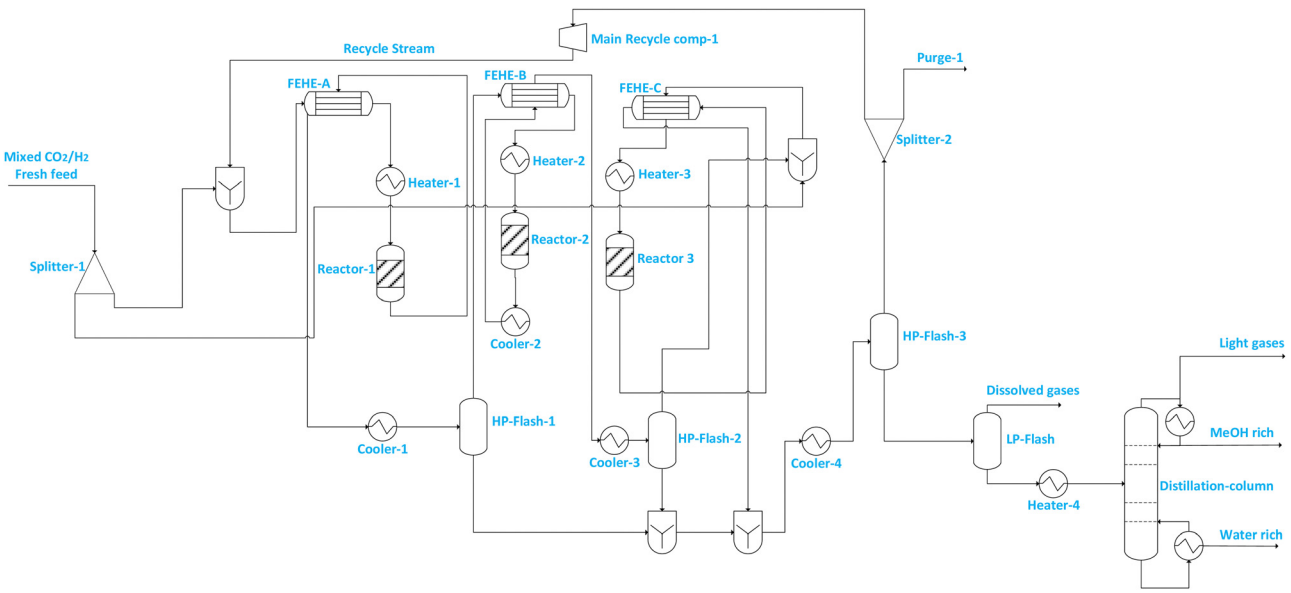

Fig. 5 Illustration of flowsheet 8. This flowsheet features three adiabatic reactors in series with intermediate cooling.

2.3. Dynamic reactor system modelling for flexibility analysis

Three of the most promising reactor configurations were selected and assessed in comparison for their flexibility analysis. The loads were varied from minimum to maximum (*i.e.*, 40–102%) with consideration of practicality in the design of the equipment such as pumps, compressors (*e.g.*, to prevent surge and stonewall), *etc.* Dynamic modelling of the methanol synthesis section is conducted using ASPEN DYNAMICS V11®. The initial state of the different reactor configurations was extracted from steady-state simulations conducted using Aspen Plus by means of a pressure driven approach leading to a more realistic model comparable to real plants. The flowsheets after dynamic translations (with all critical control loops) are shown in Section A4.1 (ESI†). The dynamics of the process are highly dependent on the reaction kinetics and modelling approaches.[34] For the dynamic simulation, the distillation section is excluded following the findings from Cui *et al.* that distillation dynamics, which affects the product quality, is easy to manage under variable loads.[66] For methanol synthesis, the feed H_2 and CO_2 were mixed at a stoichiometric

ratio of $H_2/CO_2 = 3$, before being mixed further with the recycle stream.

Signal generators were used during the dynamic modelling, to alter the rates of flow change (*i.e.*, load change) for the feed gases. Moreover, tuned proportional–integral (PI) controllers were used for dynamic operation. The proportional and integral gains were tuned based on the Ziegler–Nichols and Tyreus–Luyben tuning rules by using the automatic controller tuning in ASPEN DYNAMICS V11®. The details of the tuned controllers are given in the ESI.† The systems are evaluated considering the KPIs such as energy efficiency, flowrate of the feed streams (*i.e.*, load change), reactor conversion, heat duties and power of the compressors. The hydrogen produced from the renewable electricity and methanol represent the major power input and output, respectively.

2.4. Technical performance indicators

The mass and energy balance of the process configurations were calculated. The selected indicators to evaluate the studied processes including the overall CO_2 conversion, energy efficiency, production rate, and load change are used as criteria for comparisons. The energy efficiency expressions of the SOEC system, and the overall system defined below, follow from the work of Lonis *et al.* and Cui *et al.*[59,60,66] For the SOEC unit operating to produce hydrogen or syngas as the key product, eqn (9) describes the expression for the efficiency of the water electrolysis section:

$$\%\,\eta_{\mathrm{SOEC,product}} = \frac{\dot{m}_{\mathrm{product}} \times \mathrm{LHV}_{\mathrm{product}}}{P_{\mathrm{SOEC}} + P_{\mathrm{BOP,SOEC}}} \quad (9)$$

where $\dot{m}_{\mathrm{product}}$ refers to the mass flowrate of hydrogen or syngas (for co-electrolysis), $\mathrm{LHV}_{\mathrm{product}}$ refers to the lower heating value of hydrogen or syngas, P_{SOEC} refers to the electric power of the SOEC while $P_{\mathrm{BOP,SOEC}}$ is the power of the SOEC auxiliaries. Single pass conversion of carbon is expressed by eqn (10). CO is considered in the calculation of single pass conversion since the feed to the reactor contains CO introduced by recycle although the overall system boundary feed to the process doesn't contain CO but only CO_2 and H_2O. The efficiency of the integrated SOEC and the methanol synthesis, *i.e.*, the PtMeOH efficiency, can be described using eqn (11):

$$\%\,\eta_{\mathrm{C,conversion}} = \frac{(\mathrm{CO}_{2,\mathrm{in}} + \mathrm{CO}_{\mathrm{in}}) - (\mathrm{CO}_{2,\mathrm{out}} + \mathrm{CO}_{\mathrm{out}})}{(\mathrm{CO}_{2,\mathrm{in}} + \mathrm{CO}_{\mathrm{in}})} \quad (10)$$

$$\%\,\eta_{\mathrm{PtMeoH}} = \frac{\dot{m}_{\mathrm{MeOH}} \times \mathrm{LHV}_{\mathrm{MeOH}}}{P_{\mathrm{SOEC}} + P_{\mathrm{BOP,SOEC}} + E_{\mathrm{MSS}} + P_{\mathrm{BOP,MSS}}} \quad (11)$$

where E_{MSS} refers to the heat energy requirements in the methanol synthesis unit (MSS), *i.e.*, for preheating the feed to the reactor and distillation column, and for reboiler in the distillation. $\dot{m}_{\mathrm{MeOH}}$ (kg h^{-1}) is the mass flow rate of the streams, LHV is the lower heating value for the gases, and P represents the heat duty of the heat exchangers or the power inputs for the recycle compressor and pumps. Furthermore, heat integration is also considered for all the most promising flowsheets and thus the composite curves and exchanger designs are investigated. Heat integration eliminates/reduces external heat requirements in the methanol synthesis and distillation section (*i.e.*, yield to $E_{\mathrm{MSS}} \approx 0$). A brief analysis of the impact of heat integration on the three selected flowsheets (flowsheets 7, 7B and 8) is presented in Section A4.3 of the ESI.†

3. Results and discussion

3.1. Electrolyser performance: steam *vs.* co-electrolysis

Table 7 summarises the energy balance pertaining to heating and cooling within the SOEC system. High temperature SOEC has an advantage in terms of having higher energy efficiency. This is because this technology utilises both heat and electricity. In general, the higher the temperature, the lower the electricity demand. On the other hand, increasing the temperature reduces the overvoltage losses, *i.e.*, the ohmic losses. Therefore, the SOEC exhausts (anode and cathode) are used to preheat and superheat the feed streams containing recirculated oxygen sweep gas and demineralized water.

An additional external heat source is still required to preheat and vaporise demineralized water, and further raise the temperature of the demineralized steam and sweep gas to the SOEC operating temperature (850 °C). Table 8 summarises the performance of the steam and co-electrolyser considering the power consumption and energy efficiency. For the steam electrolysis-based SOEC required to produce about 1213 kmol h^{-1} of hydrogen under the operating conditions

Table 7 Energy balance in the SOEC section under steam electrolysis

Heating process	Heat (kW)	T_{in} (°C)	T_{out} (°C)	Cooling process	Heat (kW)	T_{in} (°C)	T_{out} (°C)
Sweep air PH by heat recovery (FEHE6)	116	248	650	Anode exhaust 1st cooling (FEHE6)	−113	850	831
Sweep air SH by an external source (Heater 3)	61	650	850	Anode exhaust 2nd cooling (FEHE4)	−1273	831	619
Water PH and VAP by external heat (Heater 1)	21 602	28	180	Anode exhaust 3rd cooling (FEHE2)	−137	619	595
Water SH by heat recovery (FEHE1)	2422	180	332	Anode exhaust 4th cooling (ANOD-COOL)	−2587	595	130
Water SH by heat recovery (FEHE2)	137	332	340	Cathode exhaust 1st cooling (FEHE5)	2110	850	707
Water SH by heat recovery (FEHE3)	2755	340	505	Cathode exhaust 2nd cooling (FEHE3)	−2755	707	515
Steam SH by heat recovery (FEHE4)	1273	505	579	Cathode exhaust 3rd cooling (FEHE1)	−2422	515	342
Water SH by heat recovery (FEHE5)	2111	579	697	Cathode exhaust 1st cooling (CAT-COOL)	−9023	342	35
Steam SH by external heat (Heater 2)	2835	714	850				

SH = super heat, VAP = vaporisation, PH = preheating.

Table 8 Performance of the electrolyser system for steam electrolysis and co-electrolysis

		Steam-electrolysis	Co-electrolysis
Parameter/index	Units	Value	Value
LHV (H_2 or CO + H_2)	MJ kg^{-1}	120	25
P_{SOEC}	MW	84	107
$P_{SOEC,BOP}$	MW	25	27
$\eta_{soec,\ system}$	%	74.5	76.2
$\eta_{soec,\ system,\ R}$	%	78.2	79.2

stipulated in Table 2, a corresponding electrical power of approximately 109 MW is required. Since the electrolyser is operated at thermoneutral voltage, the efficiency is high due to negligible overpotential losses compared to endothermic operation.[55] The steam-based SOEC system efficiency value of $\eta_{soec,system}$ = 74.5–78.2% obtained in this work is comparable to values that have been reported in the literature for the SOEC efficiency values[52,53,55,56] at thermoneutral voltage such as the value ($\eta_{soec,sytem}$ = 83%) which was presented in the work of Lonis *et al.*, who used the definition of energy efficiency similar to eqn (9) above, even though the model for SOEC was fairly simplified in this work.[60] The slight under-estimation of efficiency in this work is perhaps due to the differences in model formulation. However, the results are very comparable to what the literature reports for SOEC energy efficiency at thermoneutral voltage,[52,53,55,56] thus giving confidence about the relevance of model formulation assumptions in this work. On the other hand, the co-electrolysis based SOEC efficiency considering the BOP energy consumption was found to be around $\eta_{soec,\ system}$ = 76–79% and comparable to the literature.[32,55] The power consumption in the co-electrolysis mode is however higher than that in the steam based SOEC mode and this trend is similar to that found by Patcharavorachot *et al.*[50] This is because in the co-electrolysis mode, both H_2O and CO_2 conversion reactions consume electrical power.[50]

However, for the co-electrolysis-based mode, a slightly higher (1.7% more than the water-electrolysis mode) overall SOEC system energy efficiency was obtained for the same ratio. This is mainly due to reduced feed steam requirements in the co-electrolysis mode, as part of the steam is produced from the CO_2 to CO reaction (*i.e.*, RWGS). It is also critical to highlight that the hot streams from the SOEC have been used only for the heating of the cold streams in the SOEC section to avoid complications of the process and to better assess the influence of the configured methanol synthesis section on the overall energy efficiency of the process. This renders the two systems thermally independent, which is advantageous when variable renewable electricity is used in PtMeOH, provided this is achieved at minimal possible cost. This allows for some degree of flexible part-load operation for each section with reduced regulation or operation issues.

As also highlighted by Chen and Yang *et al.*, integration of heat between two or more subsystems should be minimized unless otherwise necessary, and optimal integration (also reducing heat curtailments) within a subsystem should be maximised.[31] For the final heating of the steam *via* heater 3, an external source is required (*e.g.* electricity) in order to achieve the operating conditions of the SOEC. An alternative would be to operate the electrolyser above the thermoneutral point and thus use the surplus heat from overpotentials, but this is not considered in this study as it adversely promotes cell degradation. External electrical heat requirements for the SOEC section (≈24% of the total electrolysis power) are needed to generate superheated steam and heat the sweep gas to the SOEC temperature. The sweep gas must first be compressed and heated to the SOEC temperature.

3.2. Methanol production rate, energy efficiency, overall and single-pass CO_2 and H_2 conversion

Comparison of the process flowsheet configurations based on the methanol production rate, energy efficiency, carbon conversion and H_2 conversion is shown in Fig. 6, Tables 9 and 10. The overall CO_2 conversion is calculated considering a recycling system in all configurations. Comparison of the methanol production rate shows that the configurations with three reactors gives higher methanol production rate. The highest methanol production rate is found for flowsheet 7B which comprises of three reactors in series with intermediate cooling and separation. Comparison of the process flowsheets (see Fig. 6) shows that the configuration expressed as flowsheet 5 has a slightly higher energy efficiency. Flowsheet 7B has a similar overall CO_2 and H_2 conversion and energy efficiency as flowsheet 7 and flowsheet 8. However, flowsheet 7B differs slightly (about 1% less) in terms of the energy efficiency compared to flowsheet 5. Table 9 shows the single pass CO_2 conversion of each reactor per flowsheet configuration. Since the process configuration of flowsheets 1 and 2 follows from the work of Van-Dal and Bouallou and Kiss *et al.* the single pass CO_2 conversion from this work is comparable to that of Van-Dal and Bouallou and Kiss *et al.* for flowsheets 1 and 2, respectively.[54,58,63] The reason that flowsheets 1 and 2 were re-modelled in this work was to ensure fair comparison using similar scale and process conditions since the original work of Van-Dal and Bouallou and Kiss *et al.* used distinct conditions and/or target production capacities and kinetics.[61,64,70] Even if the capacities were to be similar, different operating conditions will yield different performance. Single pass conversion in series reactors with intermediate cooling shows an increasing trend as reactor stages increase. This is so as the removal of water and methanol *via* intermediate cooling and separation increases the driving force of the CO_2 conversion reaction and thus enhances CO_2 conversion. Although flowsheet 2 can produce a high methanol comparable to flowsheets 7, 7B and 8, it has a slightly lower energy efficiency.

Despite efforts to recover as much methanol as possible in flowsheet 4 with additional separation *via* the solvent wash column, the overall methanol production and energy efficiency is not improved for this process. This is because of thermodynamic limits on recoverable methanol in a given stream. This process may also introduce losses of valuable reactants that may otherwise be recycled and reconverted. For parallel

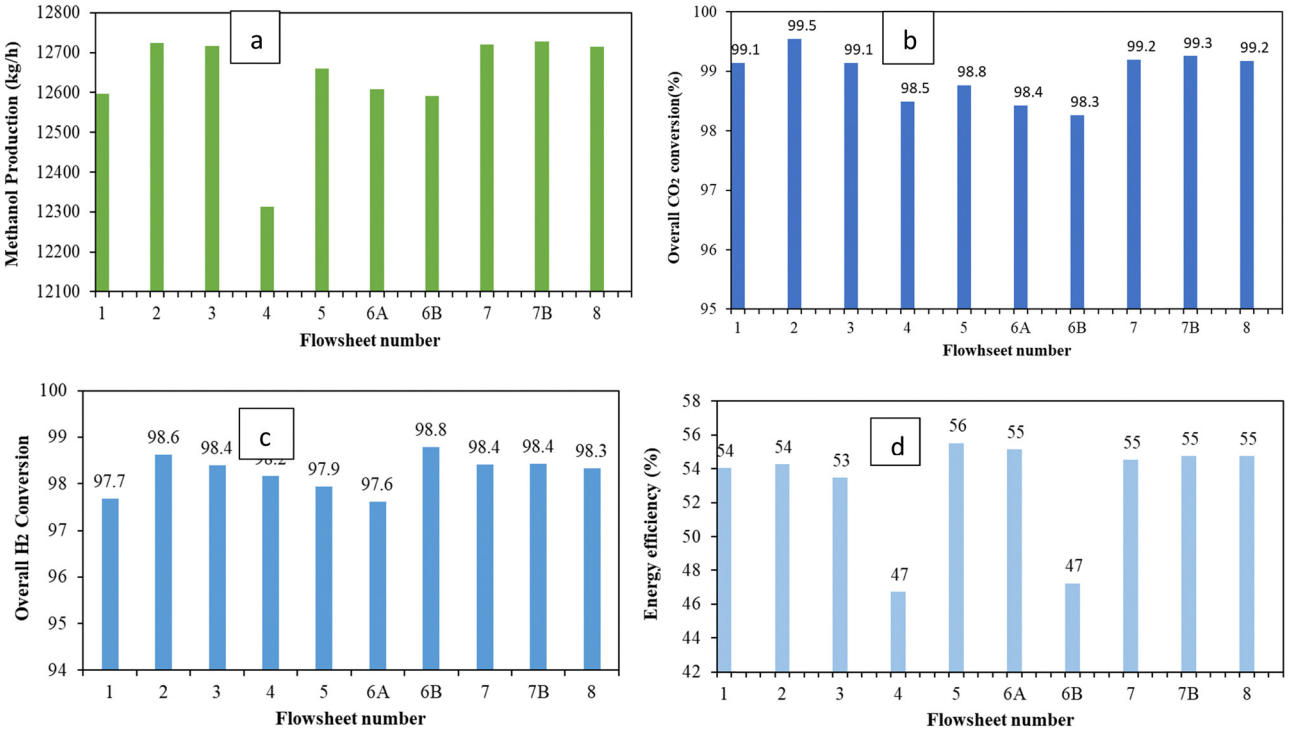

Fig. 6 Performance of the different flowsheets considered in this paper: (a) methanol production, (b) Overall CO_2 conversion, (c) overall H_2 conversion and (d) overall energy efficiency of the process.

Table 9 Single pass carbon conversions of each reactor in the evaluated process configurations

	Flowsheet number									
	1	2	3	4	5	6A	6B	7	7B	8
Reactor (R)	% CO_2 conversion in each reactor in the flowsheet									
R1	39.1	17.8	39.7	39.0	40.4	42.0	47.4	51.5	32.8	30.3
R2	—	—	53.6	53.9	55.8	42.0	10.1	51.5	42.8	40.3
R3	—	—	—	—	—	—	—	34.5	50.2	46.6

Table 10 Single pass H_2 conversions of each reactor in the evaluated process configurations

	H_2% conversion per flowsheet number per reactor									
	1	2	3	4	5	6A	6B	7	7B	8
R1	9.3	18.6	8.6	9.2	9.2	9.2	8.1	7.0	11.1	11.2
R2	—	—	6.7	7.0	6.5	9.2	4.3	7.0	9.6	10.0
R3	—	—	—	—	—	—	—	10.2	7.6	7.5

reactors having a short recycle stream, similar to the configuration in flowsheet 6B, a slight decrease in the overall methanol production rate and CO_2 conversion is observed. The short recycle also results in large recycle stream and hence increased recycle compressor duty. This decreases the energy efficiency and hence flowsheet 6B has low energy efficiency as indicated in Fig. 6d. When these parallel reactors are designed with a long recycle (flowsheet 6A) and equally divided feed, each reactor has a single pass conversion slightly higher than flowsheet 1 and flowsheet 2 which is expected because a smaller mole flowrate of the reactants is fed for comparable catalyst mass inside these reactors, thus resulting in higher residence time and hence increased carbon conversion.

The trend of conversion with changes in flowrate is also observable when reactors are staged in series with intermediate cooling. The rapid increase in the conversion of R3 corresponding to flowsheet 7B is a result of significant reduction in its feed flow-rate since the series staging of the reactors converts more of the reactants (overall, each reactor in the earlier stages receives higher flows) and the subsequent intermediate segregation of methanol and water which increases the driving force on reactor R3. In addition, the analysed process conversion is higher due to the absence of impurities in the feed. The results are comparable to the findings of Basonde and Urakawa, who experimentally demonstrated a similar single pass CO_2 conversion using 10 : 1 H_2/CO_2 feed.[71] The performance that would be achieved with 3.333 times more hydrogen (expensive to make from electrolysis) than the stoichiometric ratio in the feed is the same as having the configurations as discussed with the H_2/CO_2 ratio of 3 : 1 in the overall feed. Thus, the reactor configuration strongly influences the conversion of CO_2 to methanol.

Hydrogen storage is another key goal of the PtMeOH process. In this regard, the storage of hydrogen is assessed in terms of the amount of hydrogen that is converted to methanol in the process. Viewed from the overall process-based hydrogen conversion as depicted in Fig. 6, methanol production using flowsheet 6B with short recycle had a higher overall H_2 conversion. This is achieved without application of hydrogen gas

recovery, *e.g.* membranes, which are often applied industrially to increase the overall conversion of hydrogen. The use of membranes was not considered in this paper due to their potential to increase the methanol production cost. Table 10 shows the single pass conversion of hydrogen to methanol. The single pass conversions of hydrogen are lower than the CO_2 single pass conversions since hydrogen is always in excess in the feed of the reactor due to a significant amount of it in the recycle.

Fig. 6 also plots the energy efficiency of the flowsheets. The trend without heat integration shows that flowsheet 5 has the highest energy efficiency followed by flowsheets 7, 7B and 8. However the production rate of flowsheet 5 is slightly lower than that of flowsheets 7, 7B and 8. This is because flowsheets 7, 7B and 8 have an additional reactor which converts more materials, contributing to their slightly higher production rate. This shows a trade-off between energy efficiency and production rate. As the production rate increases, the energy efficiency decreases slightly. For flowsheet 5, the intermediate flash drums for separation of methanol and water from unconverted gases are operated at high pressures. This in effect reduces the energy requirements and size of the compressors to the second reactor and recycle. This depicts a trade-off between compression cost and flash drum pressure as observed by Luyben *et al.*[9] This implies that caution must be taken to avoid increasing pressure excessively in a way that the contents of unconverted gases and inert gases in the liquid stream sent to the distillation column increase (thus reducing the quality of the product) or significantly reducing the pressure and thus increasing the compression requirements of the recycle compressor. Flowsheets 7, 7B and 8 have the same energy efficiency (see Table 11). Thus, this indicates a trade-off between production rate and energy requirements which has been articulated by several other authors.[22,56] However, looking at the temperature profile at the exit of the reactor in flowsheets 7, 7B, and 8, opportunities for heat integration exist and could improve the energy efficiency of the process. Mechanical work and process heating (excluding the integrated heating) in this work are powered by electricity only. Energy efficiencies are still low, and this indicates the need to perform heat integration analysis and heat exchanger network design which is summarily performed and discussed in Section A4.3 of the ESI.† Before performing heat integration, sensitivity-based optimisation of the reactor section of the flowsheets is investigated for flowsheets 7, 7B and 8 to determine the optimal operating conditions associated. The results of the design sensitivity are shown in Section A4.2 of the ESI.† Sensitivity analysis of key parameters that affect the methanol synthesis process such as the recycle ratio, fresh feed partitioning, reactor feed temperature, separator pressure and temperature was performed. The findings show that fresh feed partitioning does not change the methanol production rate but can influence the control of the hot spot temperature and offer a degree of freedom under dynamic operation. From the heat integration, the series–series configuration showed low utility requirements upon optimisation of the heat exchanger network.

Table 11 Comparison of the energy efficiency obtained from this study and that found in the literature

Reference	Energy efficiency (%) w/o heat integration
Hank *et al.*[12]	40.2–44.1
Rivera Tinoco *et al.*[14]	54.8
Szima and Cormos[72]	53.93
Bos *et al.*[15]	50
Parigi *et al.*[73]	58.8
This study	Flowsheet 5: 56 Flowsheet 7: 55 Flowsheet 7B: 55 Flowsheet 8: 55

3.3. Assessment of flexibility of the methanol synthesis section

3.3.1. Feed flowrate and product streams. Generally, reactor configurations influence the flexibility of the process.[32] In this section, both parallel–series and series–series based configurations are assessed. Both series- and parallel–series-based configurations with three reactors are modelled under dynamic conditions by changing the load (feed flowrate). Simultaneous modulation of the CO_2 and H_2 feed is performed to maintain the $CO_2:H_2$ ratio of 1 : 3 in the feed. In a cascade series–series reactor design (*i.e.*, flowsheets 7B and 8 and syngas-based flowsheet), changes in the conversion and temperature in one stage influence the reaction rate of the next stage. The nonlinear relationship of temperature and concentration may render some intermediate load points infeasible, even though the minimum and maximum may be feasible. However, this was found not to be the case for all the four designs considered in the present study. The minimum and maximum loads used in this study are β_{min} = 40% and β_{max} = 105% for flowsheets 7, 7B and 8. On the other hand, the syngas-based flowsheets had a minimum allowable load-change of 45% of the nominal. Below these β_{min} values, the Aspen Dynamics integrator fails. The part-load refers to 50% of the nominal load. In this study, a load ramp (R) of 60% load per hour and a total time on stream of 15 hours were considered. Fig. 7 shows the effect of load change from full-load to part-load on the flowrates of the main feed and product streams. A linear decrease in the flowrate from full-load to part-load occurs for t = 1–2.19 h and a linear increase in the flowrate from part-load to full-load occurs for t = 5–9.51 h. This is desirable as it promises quick and good response to process variability under intermittent renewable energy. As expected, following the previous study on a single reactor by Cui *et al.*, both the methanol production rate and the purge stream follow the same trend of the load change.[66]

All three configurations had relatively comparable process flexibility, meaning they all achieved/tolerated minimum to full load operation without any violation of path constraints such as maximum allowable temperature in the reactors. However, it took 1.08, 1.16 and 1.19 h to reach the part-load steady state for flowsheets 7, 7B and 8, respectively. To reach the full load steady state from the part-load conditions, it took 1.51, 3.21 and 4.51 h for flowsheets 7, 7B and 8, respectively. Small

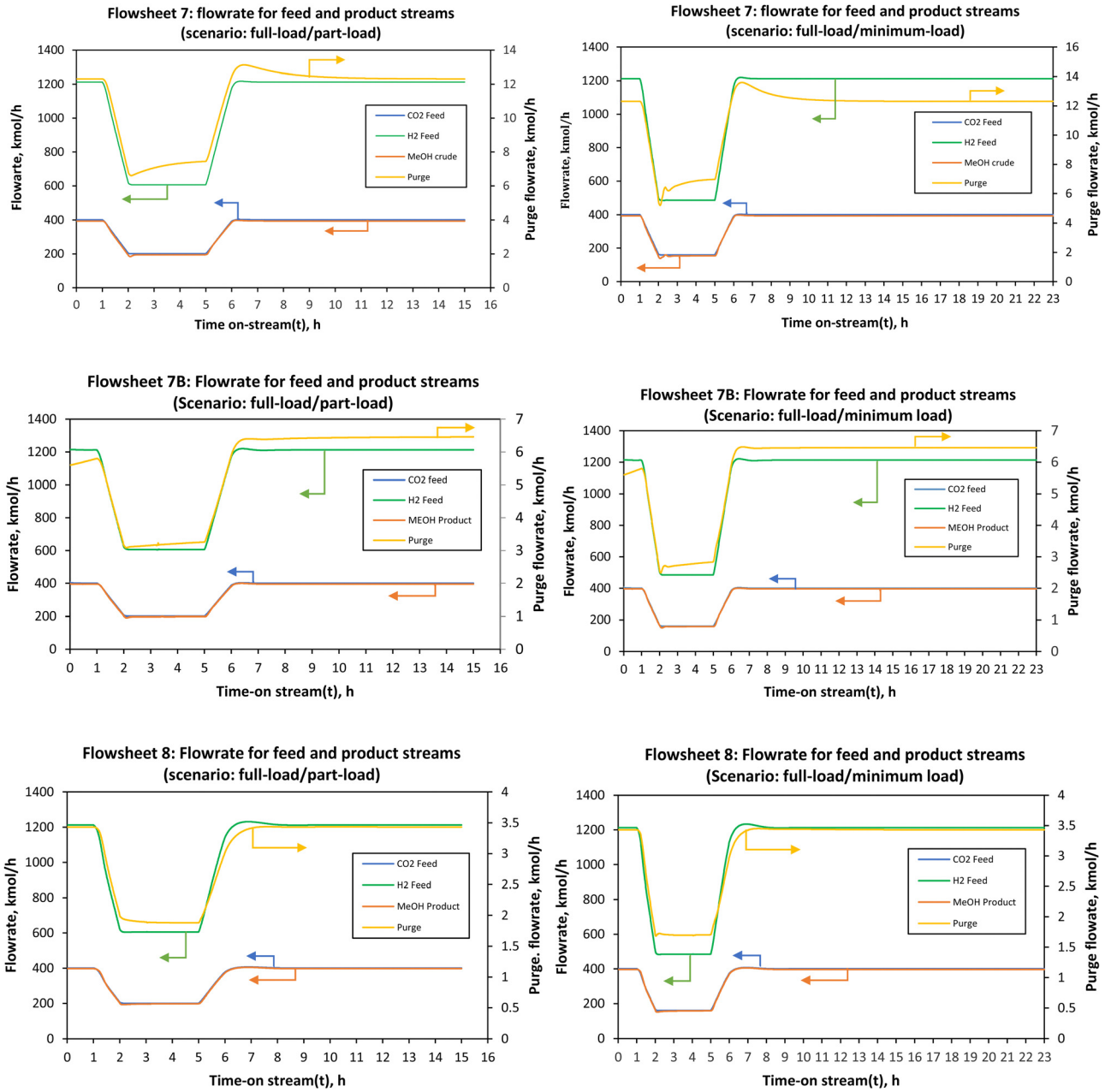

Fig. 7 Flowrate of the feed and the product streams when the load was changed from full-load (100%) to part-load (50%) and minimum load (40%). These results are for flowsheet 7, flowsheet 7B and flowsheet 8.

undershoots and overshoots are observed on the purge stream for all flowsheets at minimum load. Although these flowsheets can handle the load change very well, the parallel–series configuration (flowsheet 7) seems to be attractive with the ability to reach steady state faster. For all flowsheets, dual control (split range control) of the recycle split ratio (see flowsheet details in the ESI†) was necessary to reach low load levels and hence dynamize the methanol synthesis section. In Fig. 7B, there is an overshoot in the purge after part-load operation and it took longer than 24 hours for the purge in this flowsheet to stabilise to the initial steady state value. When comparing the CO_2 hydrogenation-based flowsheet to the syngas-based flowsheet as depicted by Fig. 8, the CO_2 hydrogenation-based flowsheet had better load flexibility than the syngas-based flowsheet, even though the architecture of the syngas-based flowsheet is similar to series–series flowsheet 8. However, operation at loads higher than nominal is possible (up to 110% for the syngas-based flowsheet).

The syngas-based flowsheet was also marred by the instability at minimum load, where undershoots were observed on the purge and syngas-feed when the load was ramped from full-load to part-load and minimum loads to full-load. It also takes a while for the recycle splitter to maintain the split ratio and hence the observed drops in the purge stream. Any flowrate

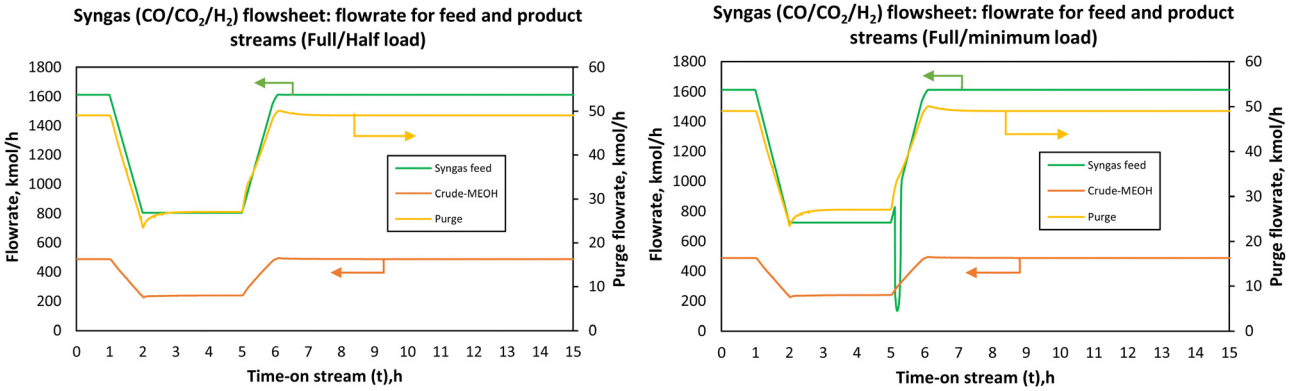

Fig. 8 Flowrate of the feed and the product streams when the load was changed from full-load (100%) to part-load (50%) and minimum load (45%) for co-electrolysis derived syngas to methanol.

within the defined load range can be reached successfully, safely and without system shutdown when the control system is properly designed. The change in the adiabatic reactors' exit temperatures with the load change was almost negligible for the CO_2 hydrogenation reaction. This is because as the feed flowrate is increased or decreased, the heat released is distributed across the reactor at higher feed flow, and the reverse water-gas shift reaction which gets more promoted at high residence time balances out the heat released at reduced flow. One would expect that with more methanol production more heat will be released in the reactors, but this is mitigated by these factors. In addition, the large recycle stream also causes the balancing effect providing the necessary temperature control and distribution. However, the potential effects of inaccuracies of the steady state kinetic model used to simulate the dynamic thermal profile must be investigated further. The current results show that the storage capacity between the methanol synthesis reactors and the upstream process (electrolysis and CO_2 capture) can be reduced at least to allow for operation in the defined load range (40–100%). Lower part-loads are expected to be problematic, more especially for the syngas-based process since the increase in residence time results in higher heat evolution inside the reactors creating the possibility of hot-spot formation. However, the final decision on the design of the feed storage capacity(s) in the upstream of the first stage reactor will be made based on the economic feasibility of each point. The economics under dynamic conditions are not considered in this study. Regardless, it is clear from the analysis in this study that methanol synthesis *via* adiabatic reactors can operate over an extended load range comparable with adiabatic reactors for methanation reaction.[32]

3.3.2. Composition of the feed. The composition of the feed of the reactor varies with load change as depicted in Fig. 9. For the parallel-series and series–series configuration, the CO_2, methanol, H_2O and CO molar content in the feed of all the three reactors decreases with the decrease in load, interestingly following the same trend as the load change.

However, the H_2 fraction in the reactor feed follows an opposite trend to load change. When the load is reduced the H_2 content at all reactor inlets increases for all flowsheets. This is attributed to the fact that much of CO_2 gets converted during the load change such that hydrogen is present in excess due to the recycle. High hydrogen content is seen in the last stage reactor. This is an interesting finding that hydrogen is in excess in the feed of the load flexible reactor during part-load. There is a slightly decreasing trend in CO_2, methanol, H_2O and CO composition for Reactor 3 in flowsheets 7 and 7B, while flowsheet 8 shows a relatively similar decrease as with other reactors.

This shows that in flowsheet 8 the concentration inertia is eliminated across the process which is required to ensure flexible operation. It takes longer hours for the composition to achieve steady state, at least for flowsheet 7 compared to flowsheet 8 and the syngas-based flowsheet, as the load changes, more especially for the last stage reactor in flowsheet 7. For flowsheet 8 and the syngas-based flowsheet, the compositions need fewer hours to return to the normal steady state after the disturbance. The parallel–series configuration (flowsheet 7) had pronounced overshoots and undershoots in the H_2 and CO_2 compositions.

3.3.3. Heat exchanger and compressor duties. Following the analysis of Fig. 10, the duties of the heat exchanger and the power of the compressors follow almost the same linear trend as the load change for all configurations. Considering the compressor duty for flowsheets 7, 7B and 8, there seems to be a similar linear decreasing trend in the power of the recycle compressor(s) with changes in load from full (100%) to part-load (50%). For example, the compressor power for flowsheet 8 decreased from 236 kW at full-load to 131 kW at part-load, which is almost a 55% decrease. This can also be attributed to the high conversion at part-load (see Fig. 12 for the trend in conversion). On the other hand, for all the coolers in the considered systems, there is an increase in the cooling duties. This trend is similar to what Cui *et al.* observed and attributed to the quality of heat in the exit streams from the reactors, *i.e.*, low grade heat of reactor effluent streams demands more cooling duty at part-load.[57] This is indeed the main energy loss for methanol synthesis as has been discussed by other authors.[57] However, the impact of effective heat integration

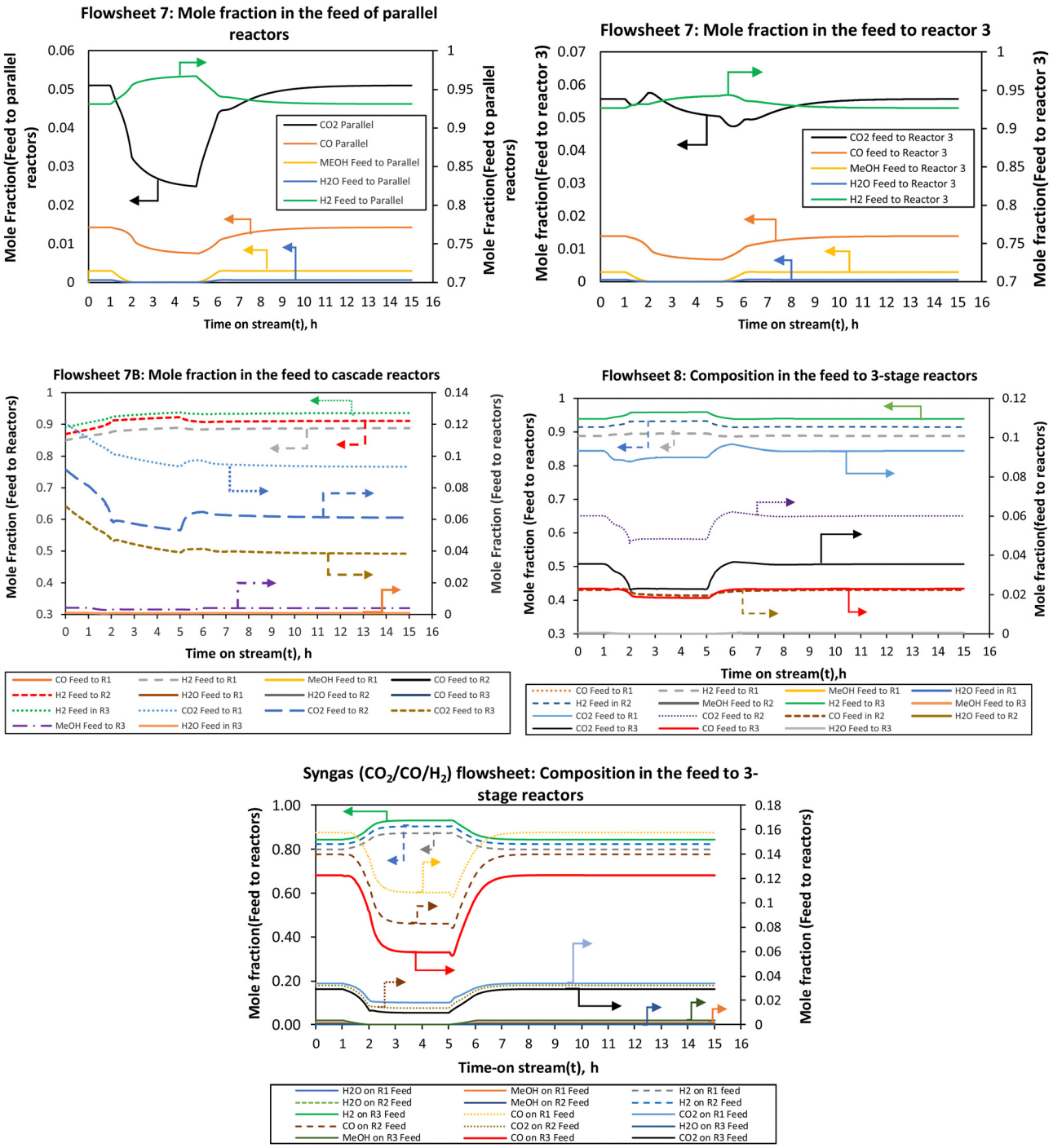

Fig. 9 The compositions of the feed streams to the reactors when the load was changed from full (100%) to half-load (50%).

(that doesn't constrain flexibility but maximises the economics of the process) must be studied. It is expected that this may reduce the cooling requirements/demands for the methanol synthesis section. Again, the thermal inertia for the considered designs seems to be negligible. However, this remains to be confirmed. The heat exchanger duties are high for parallel–series flowsheet 7 compared to the series–series configuration and the lowest exchanger duties are found in the syngas-based configuration, more especially for the heaters. For all configurations, no unfeasible heat exchanger duties (*e.g.*, negative duties for the reactor preheaters) were observed.

3.3.4. Load dependent energy efficiency. To assess the load dependency of the energy efficiency of the three methanol synthesis configurations, a case without heat integration (no feed effluent heat exchange (FEHE) was simulated) and a case with minimum reactor outlet-feed heat integration (HI) (*via* hypothetical FEHE) were assumed. The trend depicted in Fig. 11 shows a more pronounced decrease in energy efficiency

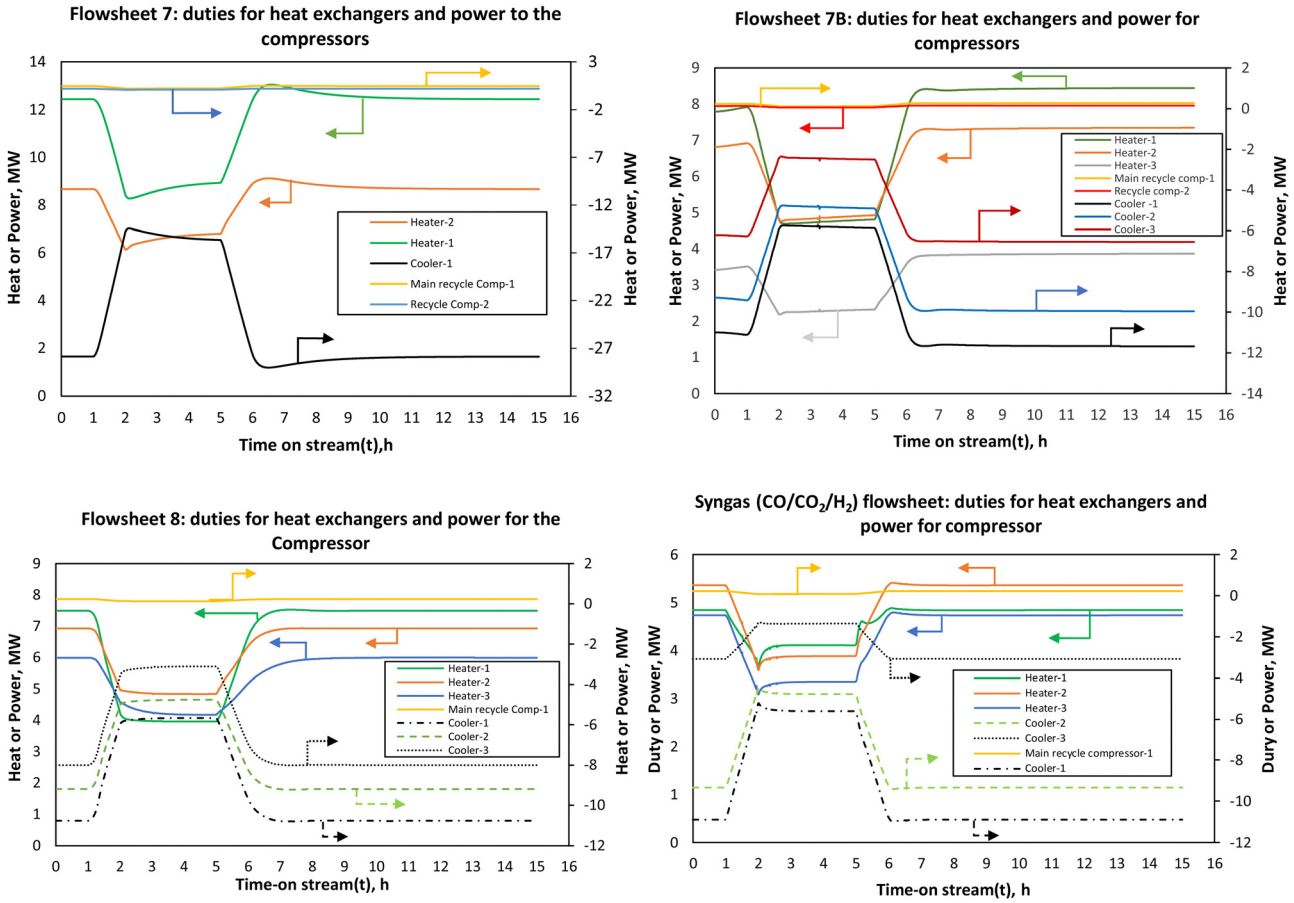

Fig. 10 The heat duties and power of the compressors to the reactors when the load was changed from full (100%) to half-load (50%).

with a decrease in the load for all the flowsheets when the heat integration *via* feed effluent (without FEHE) is not considered. For flowsheets 7 and 8, when the heat required to raise the temperature of the feed stream(s) to the reactor(s) feed was set to zero (assuming there could be heat integration using FEHE), the energy efficiency shows a very small variation from the full-load to all load levels (maximum, intermediate and minimum).

For flowsheets 7B and 8, the energy efficiency is almost stable at steady state/full load energy efficiency when this minimum heat integration is considered. Although this heat integration is necessary to improve the energy efficiency, in a real system it may induce thermal oscillations due to tight coupling with the reactor. The assumption of a perfect (hypothetical) FEHE per reactor stage shows that enhancement of thermal dynamics is expected to improve the energy efficiency of the PtMeOH system. This will be more necessary and advantageous for the coupled methanol synthesis and the upstream process (electrolysis) at higher ramping rates since it is expected that the energy efficiency of the electrolysis will increase at low load, hence potentially increasing the overall energy efficiency of the coupled system.

The findings on the energy efficiency trend for flowsheets 7 and 8 are similar to the recent finding that for a direct methanol synthesis reactor, dynamic modelling studies suggest that for part-load production capacity the energy efficiency does not decrease significantly as also deduced by Cui *et al.*[66] The energy efficiency of the methanol synthesis system in flowsheet 8 is higher than the other flowsheets. This effect is however dampened by the electrolysis and distillation units when the overall integrated steady state simulation was considered in Fig. 6 but it is expected to be more pronounced when effective heat integration is considered. For the syngas-based route, the load dependent energy efficiency is found to be lower than the other CO_2 hydrogenation systems, more especially when compared to flowsheet 8. The energy efficiency fluctuates significantly with the decrease in the load. At loads above the nominal, the energy efficiency doesn't change significantly.

3.3.5. Single pass conversion. Conversion changes with load change. As illustrated in Fig. 12, at part-load, the conversion is higher than the conversion at full-load for all the configurations. This is expected as the reduction in flowrate increases the residence time inside the reactor(s) and hence a positive step change in conversion results.

The increase is slightly higher for the parallel–series configuration in the parallel reactors (R1 and R2) due to their capacity and the fact that each feed to these reactors is further decreased, *i.e.*, split by 50%, and thus further rendering these reactors to operate at higher residence time than R3 and in

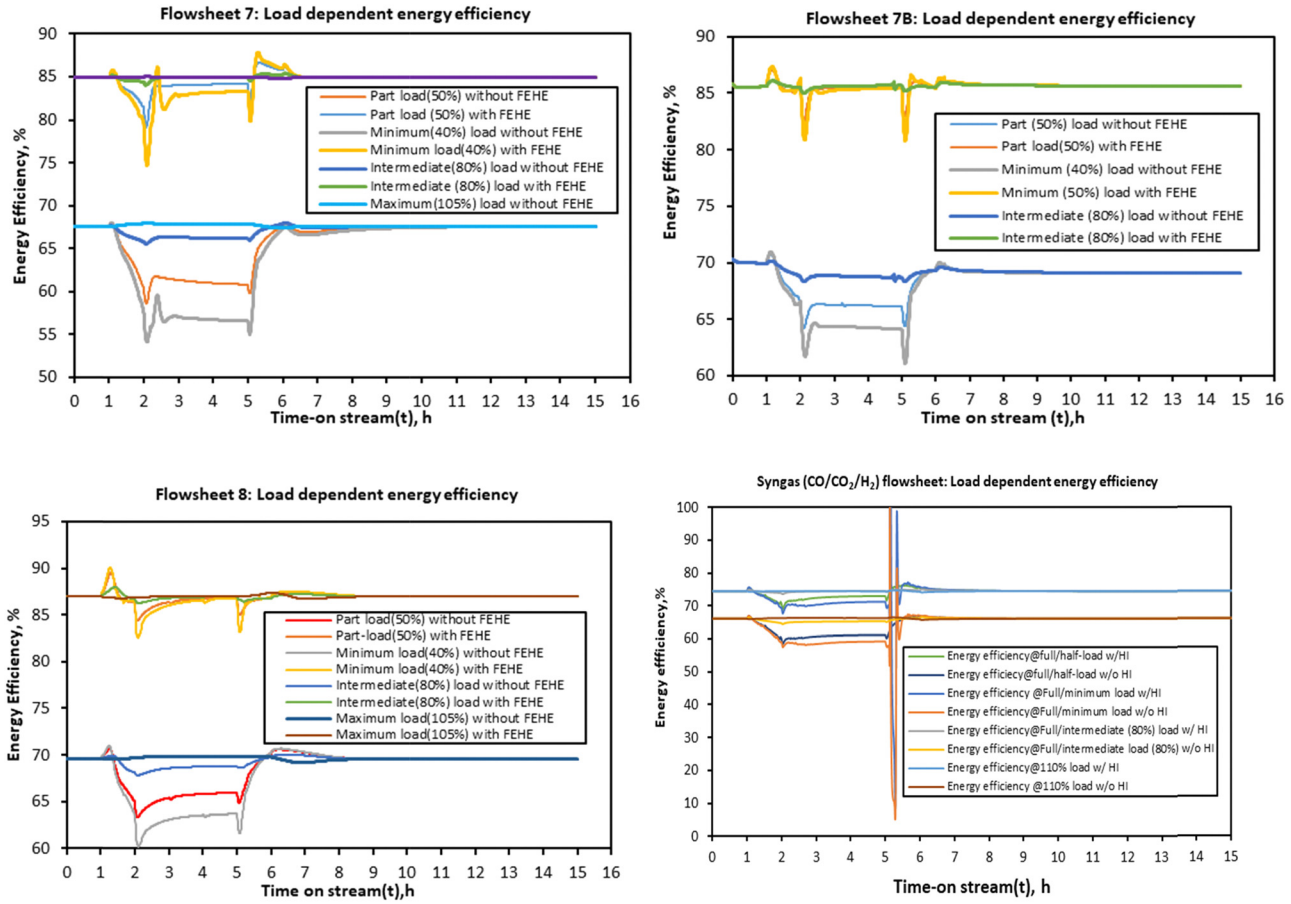

Fig. 11 The energy efficiency of the three configurations when the load was changed from full (105%) to half-load (50%), intermediate load (80%), and minimum load (40%). The ramp rate was kept constant at 60% load per hour.

contrast to R1, R2 and R3 of both configurations 7B and 8 and the syngas-based flowsheet. For CO_2 hydrogenation-based flowsheets 7B and 8, conversion increases from the first stage to the last stage, with the last reactor stage having the highest single pass conversion compared to other reactors. However, the trend is opposite for the syngas-based reactor system. The second stage reactor has the highest conversion followed by the first stage and the last stage reactor.

3.4. Comparison of the CO-rich route based on e-RWGS and Co-electrolysis-based process to the optimal CO_2 rich PtMeOH route

Production of CO-rich syngas can be done by using either a RWGS reactor or SOEC *via* co-electrolysis. Co-electrolysis offers a resource-saving and regenerative alternative to conventional syngas production.[74,75] The syngas delivered by co-electrolysis can be easily varied by changing the ratio of CO_2/H_2O and it is in the range (H_2 : CO at 1 : 1 to 3 : 1) desired for methanol synthesis. For fair comparison, the syngas feed coming from the electrolysis and e-RWGS was adjusted to 25.4/5.0/69.2% of $CO/CO_2/H_2$ with 0.4% H_2O to ensure a similar methanol production rate as the CO_2 based process while maintaining the syngas ratio of 2.1. Co-electrolysis is currently investigated in the current second phase of the Kopernikus project "P2X" at the Energy Lab 2.0 at the Karlsruhe Institute of Technology (KIT).[74] Herein the energy efficiency of co-electrolysis is compared to the optimal direct PtMeOH process and the process with e-RWGS. Recently, Haldor Topsoe has highlighted its interest in developing a renewable energy electrified reverse water gas shift reactor (e-RWGS).[76,77] The utilization of an e-RWGS reactor in methanol synthesis follows the CAMERE process relying on fire heated RWGS reactors.[76] Basini *et al.* evaluated the potential of this step but never compared it to other trending technologies such as co-electrolysis and CO_2-based PtMeOH overall processes under similar basis.[76] This section will discuss this comparison as it was modelled in this work. The SOEC-based co-electrolysis and steam electrolysis with and without e-RWGS are compared.

Following from Fig. 13, the co-electrolysis-based process has the highest energy efficiency followed by the SOEC steam electrolysis-based CO_2-hydrogenation and lastly the e-RWGS process. This is because the syngas produced from co-electrolysis in the SOEC has a higher heating value and the SOEC uses less heat under co-electrolysis compared to steam electrolysis despite the co-electrolysis having higher electricity consumption.[50]

However, following from previous analysis, co-electrolysis may be flexible in terms of feed stock but for regions with

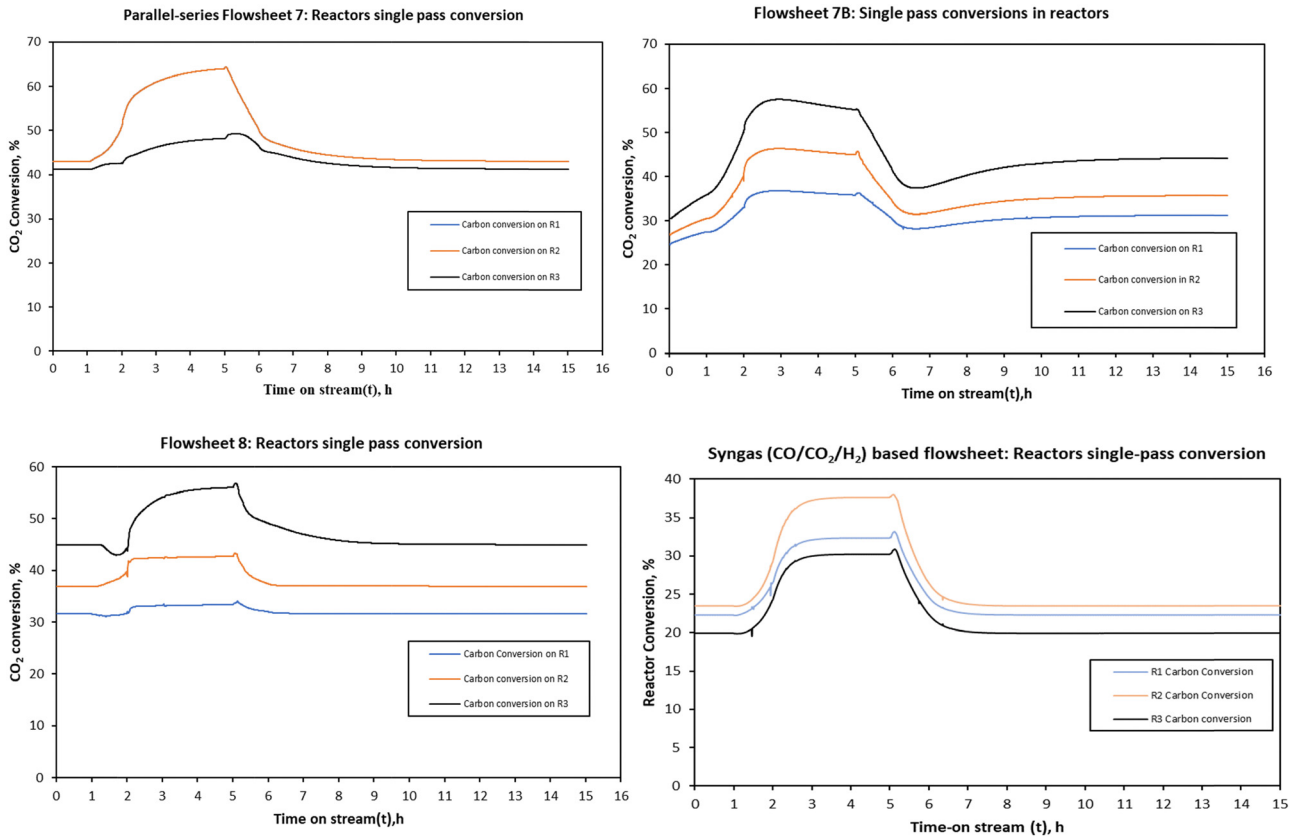

Fig. 12 The single pass reactor conversion for the three system configurations when the load was changed from full (105%) to half-load (50%).

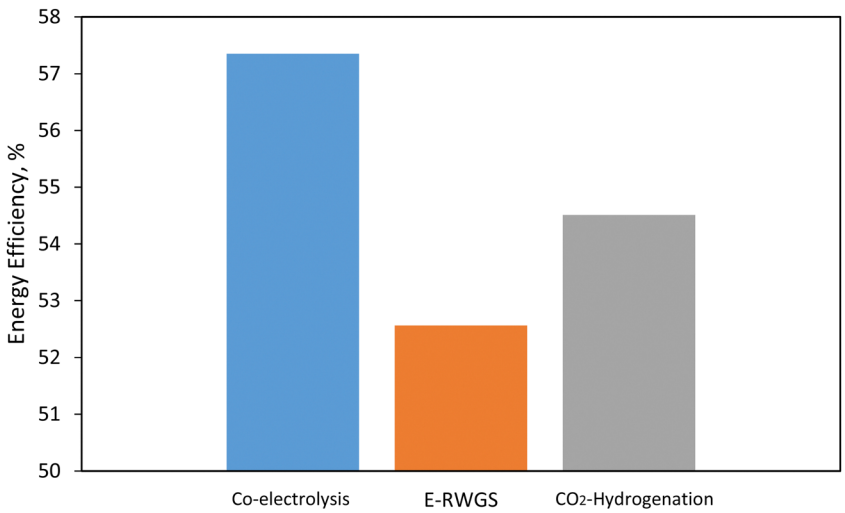

Fig. 13 Energy efficiency comparison of co-electrolysis, e-RWGS, and CO_2 based power to methanol process.

largely fluctuating electricity up to very low loads, steam electrolysis-based methanol is recommended than the co-electrolysis-based process due to the higher flexibility range of the CO_2 hydrogenation-based methanol process and the low power requirements for the SOEC steam electrolysis compared to SOEC-based co-electrolysis as discussed in Section 3.1. However, other factors may come into play such as the site-specific conditions, CO_2 emission reduction targets of the process and desired production rates.[78,79]

4. Conclusions

This work has compared twelve different SOEC-based power-to-methanol process configurations. The performance of the SOEC

under steam- and co-electrolysis-based operation was first modelled and compared. The results show that steam electrolysis uses less power than co-electrolysis. However, the co-electrolysis based SOEC leads to the highest energy efficiency. Following from this, different adiabatic reactor configurations based on CO_2 hydrogenation were compared. Among these configurations, parallel–parallel, parallel–series and series–series based configurations were integrated with the SOEC unit operating under steam electrolysis and compared considering the overall energy efficiency, conversion, production rate, and single pass conversion profiles. Three candidate process flowsheets featuring parallel–series and series–series based configurations were selected for further comparison. The selected parallel–series configurations (flowsheet 7) feature three reactors in which the first two are in parallel and in series with the third adiabatic reactor.

The selected promising series–series configuration (flowsheets 7B and 8) features three reactors in series with intermediate cooling and separation. Thereafter the sensitivity-based analysis or optimisation and heat integration are performed on the most promising flowsheets. The series–series configuration showed low utility requirements upon optimisation of the heat exchanger network. To further assess the potential of these configurations, dynamic simulation was performed using Aspen Dynamics to assess their flexibility in terms of load change and considering parameters such as load change flexibility range, time to steady state, composition changes, heat duty, power of the main units, load dependent energy efficiency, and single pass reactor conversion profile. The dynamic simulation also featured the comparison of CO_2 hydrogenation-based and syngas (derived from co-electrolysis) based flowsheets. Time to reach steady state was shorter for the parallel–series configuration compared to the series–series configuration but the allowable load flexibility range (40–105%) is similar for all the three CO_2-based configurations. This indicates the potential to reduce the size of the intermediate product storage (*e.g.*, H_2 storage) and allow more flexible direct coupling of the electrolysis and methanol synthesis sections. The syngas-based flowsheet, although similar in architecture to the CO_2 hydrogenation-based flowsheet 8, cannot be ramped down to below 45% of the nominal load. Flowsheet 8 had the highest load dependent energy efficiency and reduced instability (undershoots and overshoots). Conversion increases with reduced load for all flowsheets. Overall, considering all factors, the series-based configuration with three adiabatic reactors in series is the most promising configuration. Multistage reactors offer the opportunity to promote flexibility by reducing the reactor overdesign, and allow for operating one reactor per time based on the available power supply and allowable idle period/downtime as may be set to prevent reactor damage and potential catalyst deactivation.

5. Future work

Future work must evaluate techno-economics of the flowsheets to better discriminate among the three candidate flowsheets for CO_2 hydrogenation. Furthermore, when the stoichiometric SOEC steam electrolysis-based integrated methanol synthesis is compared to co-electrolysis-based and e-RWGS-based configurations, e-RWGS showed worse performance in terms of energy efficiency.

Although it has been demonstrated in this work that the reactor configuration plays an important role in the performance of the dynamic power-to-methanol process, especially when the high efficiency electrolyser technology is used, more work is required to understand the dynamic operation strategies such as cold start-up, warm-standby, hot-standby and shutdown, and their effect on degradation and profitability of the process. For example, in the case of power-to-methanol operated with variable electricity, the reactor may need to be kept at stand-by mode to avoid condensation for example by recirculating the feed by means of bypassing the separator and shutting the purge thereby creating a batch system. Due to the enormous amount of energy required by the power-to-methanol *via* CO_2 hydrogenation, opportunities exist to further optimise the energy efficiency of the system with the intermediate product storage included. This must be assessed.

From the dynamic flexibility study conducted for the methanol synthesis section in this paper, it emanates that power to methanol will offer both flexibility and long-term energy storage in future markets. More data on hydrogen production are needed to further optimize the process. Future work should consider effects of perturbation of the feed conditions on the dynamics of the hot-spot temperature and methanol production from the low-cost adiabatic reactor as may be prevalent in the cases where variable power is used in the power-to-methanol process. This includes variation of the H_2-to-CO_2 ratio. The H_2-to-CO_2 ratio may be a major manipulable parameter in the case when renewable energy is used in the power-to-methanol system. In this study, CO_2 is assumed continuous and thus dynamic effects as well as the associated CO_2 storage are not considered. Future work should also consider the comparison of the heat integration potential when using the water-cooled reactor which generates medium pressure steam against the adiabatic reactor in the case of power-to-methanol, in particular the steam utilization effect of coupling medium pressure steam to SOEC. This should also consider the thermal inertia in the catalyst and its effect on the process performance. In addition, because of different loads, the time co-ordination of heat recovery between various heat sources and sinks must be assessed as well as its associated economics and energy efficiency. This study considered constant pressure drop in the reactor. It would be necessary to consider variation in the pressure drop and the effect of modifying the reactor design, *e.g.*, internals, on the optimization of the proposed load flexible design. Future work should also consider integrating the stochastic forecasting market model to the flexible process for advantageous response to different electricity prices and methanol selling prices. This can also be coupled with methanol fuel cells. In this work, simplified models were used to study the best configuration with minimal complexity and thus future work must consider more detailed (*e.g.* 2D) models

including improved kinetic models (formulated with dynamic experimental conditions as well as non-negligible heat and mass transport) for better optimisation of the load flexible reactor configuration while considering the sample electricity variation cycle and its corresponding H_2 and CO_2 production from the coupled electrolysis and capture processes, respectively. Other intensification methods such as structured reactors/catalysts must also be investigated and compared. It would also be interesting to understand the significance of methanol reactor dynamics on the overall integrated efficiency of the PtMeOH process and quantify the benefit in terms of the overall plant availability.

Data availability

The data that support the findings of this study are available from the corresponding author upon reasonable request.

Nomenclature

Symbol	Meaning (unit)
AWE	Alkaline-water based electrolyser (−)
b_i	Logarithmic Arrhenius constants (−)
e-RWGS	Electrified reverse water gas shift reactor
ΔG	Gibbs free energy (J mol^{-1})
ΔH_r	Heat of reaction (kJ mol^{-1})
COR	Carbon oxide ratio (−)
$GHSV_0$	Gas hourly space velocity under nominal standard conditions (h^{-1})
GHSV	Gas hourly space velocity (NL h^{-1} gcat^{-1})
HEN	Heat exchanger network
LCOM	Levelised cost of methanol ($ per tMEOH)
k_j	Reaction rate constant (–)
K_i	Adsorption constant (–)
M_{w_i}	Molecular weight (kg mol^{-1})
m_c	Mass of the catalyst (kg)
m_i	Mass of the component (kg)
PteMeOH	Power to methanol
R	Ideal gas constant (J mol^{-1} K^{-1})
RKSMHV2	Redlich–Kwong–Soave with modified Huron–Vidal mixing rules
SN	Stoichiometric number (−)
T	Temperature (K)
SOEC	Solid oxide electrolyser (−)
ε	Fixed bed porosity (−)
ρ_{cat}	Catalyst density (kg m^{-3})

Conflicts of interest

The authors declare that they have no known competing financial interests or personal relationships that could have appeared to influence the work reported in this paper.

Acknowledgements

This work was supported by the South African Department of Science and Innovation (DSI) for research activities under the HySA Infrastructure Centre of Competence (KP5 program, Project No. CNMH17X) and by the Council for Scientific and Industrial Research (CSIR) (Project No. C1GEN25, C8GOH26).

References

1 N. Salmon and R. Bañares-Alcántara, Green ammonia as a spatial energy vector: a review, *Sustainable Energy Fuels*, 2021, **5**(11), 2814–2839.
2 S. Giannoulidis, V. Venkataraman, T. Woudstra and P. V. Aravind, Methanol based Solid Oxide Reversible energy storage system–Does it make sense thermodynamically?, *Appl. Energy*, 2020, **278**, 115623.
3 C. Hank, A. Sternberg, N. Köppel, M. Holst, T. Smolinka, A. Schaadt, C. Hebling and H. M. Henning, Energy efficiency and economic assessment of imported energy carriers based on renewable electricity, *Sustainable Energy Fuels*, 2020, **4**(5), 2256–2273.
4 E. Moioli, R. Mutschler and A. Züttel, Renewable energy storage via CO_2 and H_2 conversion to methane and methanol: Assessment for small scale applications, *Renewable Sustainable Energy Rev.*, 2019, **107**, 497–506.
5 R. Y. Chein, W. H. Chen, H. C. Ong, P. L. Show and Y. Singh, Analysis of methanol synthesis using CO_2 hydrogenation and syngas produced from biogas-based reforming processes, *Chem. Eng. J.*, 2021, 130835.
6 Y. Zheng, S. You, X. Li, H. W. Bindner and M. Münster, Data-driven robust optimization for optimal scheduling of power to methanol, *Energy Convers. Manage.*, 2022, **256**, 115338.
7 A. González-Garay, M. S. Frei, A. Al-Qahtani, C. Mondelli, G. Guillén-Gosálbez and J. Pérez-Ramírez, Plant-to-planet analysis of CO_2-based methanol processes, *Energy Environ. Sci.*, 2019, **12**(12), 3425–3436.
8 D. Vázquez and G. Guillén-Gosálbez, Process design within planetary boundaries: Application to CO_2 based methanol production, *Chem. Eng. Sci.*, 2021, 116891.
9 W. L. Luyben, Design and control of a methanol reactor/column process, *Ind. Eng. Chem. Res.*, 2010, **49**(13), 6150–6163.
10 A. Hankin and N. Shah, Process exploration and assessment for the production of methanol and dimethyl ether from carbon dioxide and water, *Sustainable Energy Fuels*, 2017, **1**(7), 1541–1556.
11 M. R. Gogate, Methanol synthesis revisited: reaction mechanisms in CO/CO_2 hydrogenation over Cu/ZnO and DFT analysis, *Pet. Sci. Technol.*, 2019, **37**(5), 603–610.
12 M. Bowker, Methanol synthesis from CO_2 hydrogenation, *ChemCatChem*, 2019, **11**(17), 4238.
13 B. Stefansson, Power and CO_2 emissions to methanol, In Presentation, 2015 European methanol policy forum 2015.

14 H. W. Lee, K. Kim, J. An, J. Na, H. Kim, H. Lee and U. Lee, Toward the practical application of direct CO_2 hydrogenation technology for methanol production, *Int. J. Energy Res.*, 2020, **44**(11), 8781–8798.
15 X. Jiang, X. Nie, X. Guo, C. Song and J. G. Chen, Recent Advances in Carbon Dioxide Hydrogenation to Methanol via Heterogeneous Catalysis, *Chem. Rev.*, 2020, **120**(15), 7984–8034.
16 H. Ruland, H. Song, D. Laudenschleger, S. Stürmer, S. Schmidt, J. He, K. Kähler, M. Muhler and R. Schlögl, CO_2 hydrogenation with Cu/ZnO/Al2O3: A benchmark study, *ChemCatChem.*, 2020, **12**(12), 3216–3222.
17 M. J. Bos, S. R. Kersten and D. W. Brilman, Wind power to methanol: Renewable methanol production using electricity, electrolysis of water and CO_2 air capture, *Appl. Energy*, 2020, **264**, 114672.
18 H. Al-Kalbani, J. Xuan, S. García and H. Wang, Comparative energetic assessment of methanol production from CO_2: Chemical versus electrochemical process, *Appl. Energy*, 2016, **165**, 1–3.
19 M. Pérez-Fortes, J. C. Schöneberger, A. Boulamanti and E. Tzimas, Methanol synthesis using captured CO_2 as raw material: Techno-economic and environmental assessment, *Appl. Energy*, 2016, **161**, 718–732.
20 H. Zhang, L. Wang, M. Pérez-Fortes, F. Maréchal and U. Desideri, Techno-economic optimization of biomass-to-methanol with solid-oxide electrolyzer, *Appl. Energy*, 2020, **258**, 114071.
21 R. Rivera-Tinoco, M. Farran, C. Bouallou, F. Auprêtre, S. Valentin, P. Millet and J. R. Ngameni, Investigation of power-to-methanol processes coupling electrolytic hydrogen production and catalytic CO_2 reduction, *Int. J. Hydrogen Energy*, 2016, **41**(8), 4546–4559.
22 H. Zhang, L. Wang, F. Maréchal and U. Desideri, Techno-economic optimization of CO_2-to-methanol with solid-oxide electrolyzer, *Energies*, 2019, **12**(19), 3742.
23 A. S. Alsuhaibani, S. Afzal, M. Challiwala, N. O. Elbashir and M. M. El-Halwagi, The impact of the development of catalyst and reaction system of the methanol synthesis stage on the overall profitability of the entire plant: A techno-economic study, *Catal. Today*, 2020, **343**, 191–198.
24 E. GhasemiKafrudi, L. Samiee, Z. M. Pour and T. Rostami, Optimization of methanol production process from carbon dioxide hydrogenation in order to reduce recycle flow and energy consumption, *J. Cleaner Prod.*, 2022, 134184.
25 *Process Systems Engineering: For a Smooth Energy Transition*, ed. E. Zondervan, Walter de Gruyter GmbH & Co KG, 2022.
26 J. M. Voß, T. Duan, C. Geitner, S. Schluter and T. Schulzke, Operating behavior of a demonstration plant for methanol synthesis, *Chem. Ing. Tech.*, 2022, **94**(10), 1489–1500.
27 D. R. Vallejo, Promoting sustainability in chemical process design using process modelling, environmental assessment and decision making, Doctoral dissertation, Imperial College London, 2021.
28 H. H. Chiou, C. J. Lee, B. S. Wen, J. X. Lin, C. L. Chen and B. Y. Yu, Evaluation of alternative processes of methanol production from CO_2: Design, optimization, control, techno-economic, and environmental analysis, *Fuel*, 2023, **343**, 127856.
29 H. Zhou, J. Wang, W. Meng, K. Wang, G. Li, Y. Yang, Z. Fan, D. Wang and D. Ji, Comparative investigation of CO_2-to-methanol process using different CO_2 capture technologies, *Fuel*, 2023, **338**, 127359.
30 B. Bruns, F. Herrmann, M. Polyakova, M. Grünewald and J. Riese, A systematic approach to define flexibility in chemical engineering, *J. Adv. Manuf. Process.*, 2020, **2**(4), e10063.
31 C. Chen and A. Yang, Power-to-methanol: The role of process flexibility in the integration of variable renewable energy into chemical production, *Energy Convers. Manage.*, 2021, **228**, 113673.
32 S. Mucci, A. Mitsos and D. Bongartz, Power-to-X processes based on PEM water electrolyzers: A review of process integration and flexible operation, *Comput. Chem. Eng.*, 2023, 108260.
33 M. Qi, D. N. Vo, H. Yu, C. M. Shu, C. Cui, Y. Liu, J. Park and I. Moon, Strategies for flexible operation of power-to-X processes coupled with renewables, *Renewable Sustainable Energy Rev.*, 2023, **179**, 113282.
34 B. Bruns, M. Grünewald and J. Riese, Optimal design for flexible operation with multiple fluctuating input parameters, *Computer Aided Chemical Engineering*, Elsevier, 2022, vol. 51, pp. 859–864.
35 Y. Qiu, B. Zhou, T. Zang, Y. Zhou, R. Qi and J. Lin, Extended Load Flexibility of Industrial P2H Plants: A Process Constraint-Aware Scheduling Approach, *arXiv*, preprint, arXiv:2203.02991, 2022, DOI: **10.1109/CIEEC54735.2022.9846329**.
36 H. Lange, A. Klose, W. Lippmann and L. Urbas, Technical evaluation of the flexibility of water electrolysis systems to increase energy flexibility: A review, *Int. J. Hydrogen Energy*, 2023, **48**(42), 15771–15783.
37 G. Li, Y. Gou, R. Ren, C. Xu, J. Qiao, W. Sun, Z. Wang and K. Sun, Realizing high-temperature steam electrolysis on tubular solid oxide electrolysis cells sufficing multiple and rapid start-up, *Ceram. Int.*, 2023, **49**(9), 14101–14108.
38 R. T. Zimmermann, J. Bremer and K. Sundmacher, Load-flexible fixed-bed reactors by multi-period design optimization, *Chem. Eng. J.*, 2021, 130771.
39 N. Salmon and R. Bañares-Alcántara, Impact of process flexibility and imperfect forecasting on the operation and design of Haber–Bosch green ammonia, *RSC Sustainability*, 2023, **1**(4), 923–937.
40 I. E. Grossmann and M. Morari, *Operability, resiliency, and flexibility: Process design objectives for a changing world*, 1983, Retrieved from: **http://shelf2.library.cmu.edu/Tech/14911087.pdf**.
41 R. Rinaldi and C. G. Visconti, Flexible operations of a multitubular reactor for methanol synthesis from biogas exploiting green hydrogen, *Chem. Eng. Sci.*, 2023, **272**, 118611.
42 T. Svitnič and K. Sundmacher, Renewable methanol production: Optimization-based design, scheduling and waste-heat utilization with the FluxMax approach, *Appl. Energy*, 2022, **326**, 120017.

43 Siemens, 2024. Retrieved from: https://www.siemens-energy.com/global/en/home/products-services/product-offerings/hydrogen-solutions.html.
44 Copenhagen Infrastructure Partners (CIP), 2021. Retrieved from: https://renewablesnow.com/news/cip-plans-power-to-x-plant-to-produce-green-methanol-764426/.
45 J. Sánchez-Luján, Á. Molina-García and J. J. López-Cascales, Optimal integration modeling of Co–Electrolysis in a power-to-liquid industrial process, *Int. J. Hydrogen Energy*, 2024, **52**, 1202–1219.
46 F. Samimi, M. Feilizadeh, S. B. Najibi, M. Arjmand and M. R. Rahimpour, Carbon dioxide utilization in methanol synthesis plant: process modeling, *Chem. Prod. Process Model.*, 2020, 1(ahead-of-print).
47 M. R. Rahimpour, S. Ghader, M. Baniadam and J. Fathi Kalajahi, Incorporation of flexibility in the design of a methanol synthesis loop in the presence of catalyst deactivation, *Chem. Eng. Technol.*, 2003, **26**(6), 672–678.
48 G. Léonard, D. Giulini and D. Villarreal-Singer, Design and evaluation of a high-density energy storage route with CO_2 re-use, water electrolysis and methanol synthesis, *Computer Aided Chemical Engineering*, Elsevier, 2016, vol. 38, pp. 1797–1802.
49 G. M. Kontogeorgis and G. K. Folas, *The EoS/GE mixing rules for cubic equations of state. Thermodynamic Models for Industrial Applications: From Classical and Advanced Mixing Rules to Association Theories*, John Wiley & Sons, Ltd, Chichester, 2010, pp. 159–193.
50 Y. Patcharavorachot, N. Chatrattanawet, A. Arpornwichanop and D. Saebea, Comparative energy, economic, and environmental analyses of power-to-gas systems integrating SOECs in steam-electrolysis and co-electrolysis and methanation, *Therm. Sci. Eng. Prog.*, 2023, 101873.
51 F. Lonis, Design, modelling, evaluation and comparison of energy systems for the production and use of renewable methanol using recycled CO2. PhD thesis, University of Cagliari, 2020.
52 Sunfire-Factsheet-HyLink-SOEC-20210303, https://www.sunfire.de/files/sunfire/images/content/Sunfire.de%20(neu)/Sunfire-Factsheet-HyLink-SOEC-20210303.pdf.
53 Sunfire-Factsheet-SynLink-SOEC-20210303, https://www.sunfire.de/files/sunfire/images/content/Sunfire.de%20(neu)/Sunfire-Factsheet-SynLink-SOEC-20210303.pdf.
54 J. B. Hansen, N. Christiansen and J. U. Nielsen, Production of sustainable fuels by means of solid oxide electrolysis, *ECS Trans.*, 2011, **35**(1), 2941.
55 H. Nami, O. B. Rizvandi, C. Chatzichristodoulou, P. V. Hendriksen and H. L. Frandsen, Techno-economic analysis of current and emerging electrolysis technologies for green hydrogen production, *Energy Convers. Manage.*, 2022, **269**, 116162, DOI: 10.1016/j.enconman.2022.116162ISSN 0196-8904.
56 L. Wang, M. Chen, R. Küngas, T. E. Lin, S. Diethelm and F. Maréchal, Power-to-fuels via solid-oxide electrolyzer: Operating window and techno-economics, *Renewable Sustainable Energy Rev.*, 2019, **110**, 174–187.
57 K. Im-orb, N. Visitdumrongkul, D. Saebea, Y. Patcharavorachot and A. Arpornwichanop, Flowsheet-based model and exergy analysis of solid oxide electrolysis cells for clean hydrogen production, *J. Cleaner Prod.*, 2018, **170**, 1–3.
58 S. Jamshidi, M. H. Sedaghat, A. Amini and M. R. Rahimpour, CFD simulation and sensitivity analysis of an industrial packed bed methanol synthesis reactor, *Chem. Eng. Process.*, 2023, **183**, 109244.
59 F. Lonis, V. Tola, M. Cascetta, S. Arena and G. Cau, December. Performance evaluation of an integrated energy system for the production and use of renewable methanol via water electrolysis and CO_2 hydrogenation, in AIP Conference Proceedings, AIP Publishing LLC, 2019, vol. 2191, No. 1, p. 020099.
60 F. Lonis, V. Tola and G. Cau, Renewable methanol production and use through reversible solid oxide cells and recycled CO_2 hydrogenation, *Fuel*, 2019, **246**, 500–515.
61 A. A. Kiss, J. J. Pragt, H. J. Vos, G. Bargeman and M. T. De Groot, Novel efficient process for methanol synthesis by CO_2 hydrogenation, *Chem. Eng. J.*, 2016, **284**, 260–269.
62 X. Cui and S. K. Kær, A comparative study on three reactor types for methanol synthesis from syngas and CO_2, *Chem. Eng. J.*, 2020, 124632.
63 K. V. Bussche and G. F. Froment, A steady-state kinetic model for methanol synthesis and the water gas shift reaction on a commercial Cu/ZnO/Al_2O_3 Catalyst, *J. Catal.*, 1996, **161**(1), 1.
64 É. S. Van-Dal and C. Bouallou, Design and simulation of a methanol production plant from CO_2 hydrogenation, *J. Cleaner Prod.*, 2013, **57**, 38–45.
65 D. Mignard and C. Pritchard, On the use of electrolytic hydrogen from variable renewable energies for the enhanced conversion of biomass to fuels, *Chem. Eng. Res. Des.*, 2008, **86**(5), 473–487.
66 X. Cui, S. K. Kær and M. P. Nielsen, Energy analysis and surrogate modeling for the green methanol production under dynamic operating conditions, *Fuel.*, 2021, **307**, 121924.
67 F. Nestler, A. R. Schütze, M. Ouda, M. J. Hadrich, A. Schaadt, S. Bajohr and T. Kolb, Kinetic modelling of methanol synthesis over commercial catalysts: A critical assessment, *Chem. Eng. J.*, 2020, **394**, 124881, DOI: 10.1016/j.cej.2020.124881.
68 Y. Slotboom, M. J. Bos, J. Pieper, V. Vrieswijk, B. Likozar, S. R. Kersten and D. W. Brilman, Critical assessment of steady-state kinetic models for the synthesis of methanol over an industrial Cu/ZnO/Al_2O_3 catalyst, *Chem. Eng. J.*, 2020, **389**, 124181, DOI: 10.1016/j.cej.2020.124181.
69 B. L. de Oliveira Campos, K. Herrera Delgado, S. Pitter and J. Sauer, Development of consistent kinetic models derived from a microkinetic model of the methanol synthesis, *Ind. Eng. Chem. Res.*, 2021, **60**(42), 15074–15086, DOI: 10.1021/acs.iecr.1c02952.
70 A. A. Kiss, J. J. Pragt, M. M. van Iersel, G. Bargeman and M. T. de Groot, *Continuous process for the preparation of methanol by hydrogenation of carbon dioxide*, *WIPO Pat.*, 2013144041, 2013.

71 A. Bansode and A. Urakawa, Towards full one-pass conversion of carbon dioxide to methanol and methanol-derived products, *J. Catal.*, 2014, **309**, 66–70.
72 S. Szima and C. C. Cormos, Improving methanol synthesis from carbon-free H2 and captured CO_2: a techno-economic and environmental evaluation, *J. CO_2 Util.*, 2018, **24**, 555–563.
73 D. Parigi, E. Giglio, A. Soto and M. Santarelli, Power-to-fuels through carbon dioxide Re-Utilization and high-temperature electrolysis: A technical and economical comparison between synthetic methanol and methane, *J. Cleaner Prod.*, 2019, **226**, 679–691.
74 B. de Hair, U. Fantz, A. Hecimovic, A. Schulz, A. Navarrete Munoz and M. Klumpp, Trend report technical chemistry 2021, *News Chem.*, 2021, **69**(6), 52–59.
75 Z. Zhan, W. Kobsiriphat, J. R. Wilson, M. Pillai, I. Kim and S. A. Barnett, Syngas production by coelectrolysis of CO_2/H_2O: the basis for a renewable energy cycle, *Energy Fuels*, 2009, **23**(6), 3089–3096.
76 L. E. Basini, F. Furesi, M. Baumgärtl, N. Mondelli and G. Pauletto, CO_2 capture and utilization (CCU) by integrating water electrolysis, electrified reverse water gas shift (E-RWGS) and methanol synthesis, *J. Cleaner Prod.*, 2022, **377**, 134280.
77 S. Thor Wismann, K. E. Larsen and P. Mølgaard Mortensen, Electrical Reverse Shift: Sustainable CO_2 Valorization for Industrial Scale, *Angew. Chem.*, 2022, **134**(8), e202109696.
78 C. Tsiklios, S. Schneider, M. Hermesmann and T. E. Müller, Efficiency and Optimal Load Capacity of E-Fuel-Based Energy Storage Systems, *Adv. Appl. Energy*, 2023, 100140.
79 I. Ioannou, S. C. D'Angelo, Á. Galán-Martín, C. Pozo, J. Pérez-Ramírez and G. Guillén-Gosálbez, Process modelling and life cycle assessment coupled with experimental work to shape the future sustainable production of chemicals and fuels, *React. Chem. Eng.*, 2021, **6**(7), 1179–1194.